Metal–Macrocycle Interaction in Phthalocyanines: Density Functional Calculations of Ground and Excited States

A. Rosa

Chemistry Department, Università della Basilicata, Via N. Sauro, 85, 85100 Potenza, Italy

E. J. Baerends*

Theoretical Chemistry, Chemistry Department, Free University,
De Boelelaan 1083, 1081 HV Amsterdam, The Netherlands

*Received April 29, 1993**

The interactions between the phthalocyanine macrocycle Pc^{2-} and the metal ions Co^{2+}, Ni^{2+} and Cu^{2+} are analyzed in detail. It is concluded that σ bonding is by far dominant, mostly due to strong charge donation from the pyrrolic nitrogen lone pairs into the empty or singly occupied (in Cu) $3d_{xy}$, with additional effects from donation into the $4p_{x,y}$ and 4s. The π bonds, consisting of back-donation from $3d_{\pi}$ into empty ring π orbitals and donation from occupied ring π orbitals into the metal $4p_z$ are rather weak, but there is a sizable contribution from polarization of the Pc^{2-} system. In CoPc and NiPc the total orbital interaction contribution (the covalent component) is about equal to the ionic component of the bond, the latter being identified as the sum of the Pauli repulsion and the attractive electrostatic interaction between M^{2+} and Pc^{2-}. In CuPc the electron in the $3d_{xy}$ acceptor orbital diminishes the orbital interaction contribution, making this the least strongly bound system. Comparison with Mg^{2+} shows that the ionic contribution is about the same but the covalent component of the bond drops by ca. 50% due mostly to the absence of the TM 3d AO's. Comparison of phthalocyanine (Pc^{2-}) to porphyrin (P^{2-}) shows that the larger hole size of P^{2-} has the following effects: (a) the orbital interactions are somewhat less effective due to smaller overlap; (b) the Pauli repulsion is diminished; (c) the electrostatic attraction is larger in spite of the larger hole size due to higher negative electron density on the smaller ring system of P^{2-}. The net effect is stronger bonding to P^{2-} than to Pc^{2-}. The photoelectron and optical spectra of CoPc, NiPc and CuPc have been calculated and compared to gas phase and condensed phase spectra.

1. Introduction

Phthalocyanines have attracted considerable interest both because of their relationship to the biologically important porphyrins and because of their intrinsically interesting spectroscopical, magnetic and electrochemical properties (we will use the abbreviations Pc = phthalocyanine and P = porphyrin). More recently they are receiving attention as versatile molecular building blocks of one-dimensional "molecular metals".[1]

In spite of a vast amount of experimental data, MPc's have not been theoretically investigated nearly as much as porphyrins, owing to the size of the molecules. Most of the theoretical studies available for MPc's are based on semiempirical models. Overall, they provide an interpretation of the bonding mechanism in terms of metal–Pc σ and π interactions and are able to reproduce most features of the optical spectra. Attempts to a more fundamental understanding of the electronic structure of MPc's by first principles calculations have been made only recently using density functional methods.[2-4]

In this paper the electronic structure of a series of MPc's (M = Mg, Co, Ni, Cu) is investigated in detail by a density functional approach with special emphasis on the study of the metal–macrocycle interactions. Our aim is to answer some interesting questions concerning the bond in this type of molecule, such as: (i) How ionic or covalent are phthalocyanine and porphyrin complexes? (ii) What is the relative strength of σ and π bonds? (iii) What is the interplay of d and s,p orbitals in the metal–macrocycle bond, and hence what is the bonding mechanism in phthalocyanine complexes where the metal does not have d orbitals available, as in the alkaline earth phthalocyanines? (iv) what is the relationship between the structural and electronic features of phthalocyanine and porphyrin ligands and their coordination properties. Although metal complexes of tetrapyrrole ligands are chemically similar, differences in the ligand framework may influence significantly the metal–macrocycle interactions. The Pc–P difference will be investigated using the electronic structure of a prototype porphyrin, NiP.

To answer the questions detailed above we made extensive use of an energy decomposition scheme (see next section) that, combined with a fragment formalism, has proven a useful tool in the analysis of bonding mechanisms in other porphyrin-like[5] and organometallic compounds.[6] This scheme allows us to separate the steric factors from the attractive orbital interaction contributions. The latter are broken up according to the irreducible representations of the point group (D_{4h}), which affords a quantitative estimate of the strength of σ and π interactions. The electronic structures of free-base phthalocyanine and porphyrin, H_2Pc and H_2P, respectively, have also been investigated as they provide a useful background for the understanding of metal–macrocycle interactions.

Finally we give an interpretation and discussion of optical and photoelectron spectra, on the basis of ΔSCF calculations.

* Abstract published in *Advance ACS Abstracts,* January 1, 1994.

(1) (a) Ibers, J. A.; Pace, L. J.; Martinsen, J.; Hoffman, B. M. *Struct. Bonding (Berlin)* **1982**, *50*, 1–55. (b) Ferraro, J. R. *Coord. Chem. Rev.* **1982**, *43*, 205–232. (c) Hoffman, B. M.; Ibers, J. A. *Acc. Chem. Res.* **1983**, *16*, 15–21. (d) Proceedings of the International Conference on the Physics and Chemistry of Low Dimensional Synthetic Metals (ICSM 84). *Mol. Cryst. Liq. Cryst.* **1985**, *120*. (e) Martinsen, J.; Pace, L. J.; Phillips, T. E.; Hoffman, B. M.; Ibers, J. A. *J. Am. Chem. Soc.* **1982**, *104*, 83–91. (f) Hoffman, B. M.; Martinsen, J.; Pace, L. J.; Ibers, J. A. In *Extended Linear Chain Compounds*; Miller, J. S., Ed.; Plenum: New York, 1983; Vol. 3, pp 459–549. (g) Palmer, S. M.; Stanton, J. L.; Martinsen, J.; Ogawa, M. Y.; Heuer, W. B.; Van Wallendael, S. E.; Hoffman, B. M.; Ibers, J. A. *Mol. Cryst. Liq. Cryst.* **1985**, *125*, 1.

(2) Kutzler, F. W.; Ellis, D. E. *J. Chem. Phys.* **1986**, *84*, 1033.

(3) Reynolds, P. A.; Figgis, B. N. *Inorg. Chem.* **1991**, *30*, 2294.

(4) Liang, X. L.; Flores, S.; Ellis, D. E.; Hoffman, B. M.; Musselman, R. L. *J. Chem. Phys.* **1991**, *95*, 403.

(5) Rosa, A.; Ricciardi, G.; Lelj, F.; Chizhov, Y. *Chem. Phys.* **1992**, *161*, 140.

(6) Rosa, A.; Baerends, E. J. *New J. Chem.* **1991**, *15*, 815 and references therein.

0020-1669/94/1333-0584$04.50/0

Phthalocyanines and porphyrins have similar optical spectra that arise primarily from $\pi \rightarrow \pi^*$ transitions within the delocalized macrocycle. The former, however, have a richer electronic spectrum, with many more metal dependent bands. This has been attributed[7] to (i) a greater delocalization of metal orbitals in Pc complexes, which enhances the intensity of charge transfer transitions involving d_π orbitals, and (ii) an additional number of low-lying empty π^* orbitals to give a greater number of allowed transitions. Our main goal is to locate metal-dependent features in the spectra. In fact, although photoemission[8-13] and optical spectra[14-18] are to first order almost identical for all Pc's, nevertheless metal dependent structures have been identified in the UV[15,17] and in the near-infrared region[18] of the absorption spectra. Contributions from d-like central metal orbitals can also be distinguished in the 0–6 eV range in the X-ray photoelectron spectra of Höchst et al.[12] A correct assignment of the metal dependent spectroscopical features is however quite difficult on experimental grounds alone, and a comparison with high-quality calculations is required.

2. Geometrical Parameters and Method

The calculations reported in this paper are based on the Amsterdam DF program package[19,20] characterized by the use of a density fitting procedure[19] to obtain accurate Coulomb and exchange potentials in each SCF cycle, by accurate and efficient numerical integration[20] of the effective one-electron hamiltonian matrix elements, and by the possibility to freeze core orbitals.[19a] The molecular orbitals were expanded in an uncontracted double-ζ STO basis set for all atoms with the exception of the 3d transition metal orbitals for which we used a triple-ζ STO basis set. As polarization functions one 4p and one 3d STO were used for transition metals and Mg respectively. The cores (Co, Ni, Cu: 1s–2p; Mg, C, O: 1s) have been kept frozen.

The LSD exchange potential and energy was used,[21] together with the Vosko–Wilk–Nusair parametrization for homogeneous electron gas correlation, including the Stoll correction for correlation between electrons of different spin.[23]

Bond energies included Becke's nonlocal correction[24] to the local exchange expression. It has been demonstrated that excellent metal–metal and metal–ligand bond energies are obtained from this density-functional based approach.[25]

In order to analyze the metal–macrocycle interaction energies, we use a method that is an extension of the well-known decomposition scheme of Morokuma.[26] The bonding energy is decomposed into a number of terms. The first term, ΔE^0, is obtained from the energy of the wave function ψ^0 which is constructed as the antisymmetrized and renormalized product of the wave functions ψ^A and ψ^B of the fragments A and B:

$$\psi^0 = NA\{\psi^A\psi^B\} \quad E^0 = \langle\psi^0|H|\psi^0\rangle$$

$$E^A = \langle\psi^A|H^A|\psi^A\rangle$$

$$E^B = \langle\psi^B|H^B|\psi^B\rangle$$

$$\Delta E^0 = E^0 - E^A - E^B = \Delta E_{elstat} + \Delta E_{Pauli}$$

ΔE^0, which is appropriately called the steric repulsion,[27,28] consists of two components. The first is the electrostatic interaction ΔE_{elstat} of the nuclear charges and unmodified electronic charge density of one fragment with those of the other fragment, both fragments being at their final positions. Usually ΔE_{elstat} is negative, i.e. stabilizing. The second component is the so-called exchange repulsion or Pauli repulsion ΔE_{Pauli}.[29,30] This is essentially due to the antisymmetry requirement on the total wavefunction, or equivalently the Pauli principle, which leads to a depletion of electron density in the region of overlap between ψ^A and ψ^B and an increase in kinetic energy.[31] It may be understood in a one-electron model as arising from the two-orbital four- (three-) electron destabilizing interactions between occupied orbitals on the two fragments. The steric repulsion term ΔE^0 is usually repulsive at the equilibrium distance since the repulsive component ΔE_{Pauli} dominates, but for charged fragments such as M^{2+} and Pc^{2-} the electrostatic attraction will dominate.

In addition to the steric repulsion term ΔE^0 there are the attractive orbital interactions which enter when the wave function ψ^0 is allowed to relax to the fully coverged ground-state wave function of the total molecule, ψ^{AB}. The energy lowering due to mixing of virtual orbitals of the fragments into the occupied orbitals is called the electronic interaction energy $\Delta E_{oi} = E[\psi^{AB}] - E^0$. This term, according to the decomposition scheme proposed by Ziegler,[32] which is very useful for purposes of analysis, may be broken up into contributions from the orbital interactions within the various irreducible representations Γ of the overall symmetry group of the system:

$$\Delta E = \Delta E^0 + \Delta E_{oi} = \Delta E^0 + \sum\nolimits_\Gamma \Delta E(\Gamma)$$

For the evaluation of the copper–phthalocyanine bond energy, we used the recently developed open shell fragment method,[33] which allows for a correct evaluation of the energy terms when one is dealing with open shell fragments, which is the case for copper.

The geometrical parameters used for CoPc and CuPc have been derived from experiment[34,35] and refer to their β-polymorphic form, the most stable one at room temperature and pressure. In the case of β-NiPc, the X-ray data[36] available are very old and inaccurate. In particular the Ni–N_p bond length (1.83 Å) appears too short in comparison with the M–N_p distances found in other phthalocyanine complexes of first row transition metals (N_p is pyrrolic nitrogen, N_b is the bridge nitrogen). Thus we used the experimental bond parameters of the partially oxidized $NiPcI_{1.0}$[37] that give a Ni–N_p distance of 1.89 Å. The partial oxidation has no measurable effect on the dimension of the phthalocyanine ring and $NiPcI_{1.0}$ bond parameters are in all respects similar to those of unoxidized phthalocyanine complexes (see ref 37). We shall assume for these systems an idealized D_{4h} symmetry. In the case of the alkaline earth complex, MgPc, for which the experimental data[38] indicate a C_{4v} structure with the metal atom 0.496 Å out of the plane of the ring we did calculations both for planar (D_{4h}) and nonplanar (C_{4v}) geometries. The assumed geometry for NiP is a D_{4h} planar projection of tetraphenylporphine coordinates determinated by Hoard et al.[39] with the nickel–nitrogen bond length taken from the X-ray work of Fleischer et al.[40]

(7) Schaffer, A. M.; Gouterman, M.; Davidson, E. R. *Theor. Chim. Acta* **1973**, *30*, 9.
(8) Eley, D. D.; Hazeldine, D. J.; Palmer, T. F. *J. Am. Chem. Soc., Faraday Trans. 2* **1973**, 1808.
(9) Hill, H. C.; Reed, R. I. *Tetrahedron* **1964**, *20*, 1359.
(10) Kock, E. E.; Grobman, W. D. *J. Chem. Phys.* **1977**, *67*, 837.
(11) Battye, F. L.; Goldmann, A.; Kasper, L. *Phys. Status Solidi B* **1977**, *80*, 425.
(12) Höchst, H.; Goldmann, A.; Hüfner, S.; Malter, H. *Phys. Status Solidi B* **1976**, *76*, 559.
(13) Berkowitz, J. *J. Chem. Phys.* **1979**, *70*, 2819.
(14) Chadderton, L. T. *J. Phys. Chem. Solids* **1963**, *24*, 751.
(15) Edwards, L.; Gouterman, M. *J. Mol. Spectrosc.* **1970**, *33*, 292.
(16) Schechtman, B. H.; Spicer, W. E. *J. Mol. Spectrosc.* **1970**, *33*, 28.
(17) Davidson, A. T. *J. Chem. Phys.* **1982**, *77*, 168.
(18) Fielding, P. E.; MacKay, A. G. *Aust. J. Chem.* **1975**, *28*, 1445.
(19) (a) Baerends, E. J.; Ellis, D. E.; Ros, P. *Chem. Phys.* **1973**, *2*, 42. (b) Baerends, E. J.; Ros, P. *Chem. Phys.* **1973**, *2*, 51. (c) Baerends, E. J.; Ros, P. *Int. J. Quantum Chem.* **1978**, *S12*, 169.
(20) (a) Boerrigter, P. M.; te Velde, G.; Baerends, E. J. *Int. J. Quantum Chem.* **1988**, *33*, 87. (b) Te Velde, G.; Baerends, E. J. *J. Comput. Phys.* **1992**, *99*, 84.
(21) Parr, R.G.; Yang, W. *Density-Functional Theory of Atoms and Molecules*, Oxford University Press: New York, 1989.
(22) Vosko, S. H.; Wilk, L.; Nusair, M. *J. Can. J. Phys.* **1980**, *58*, 1200.
(23) Stoll, H.; Golka, E.; Preuss, E. *Theor. Chim. Acta* **1980**, *29*, 55.
(24) Becke, A. D. *J. Chem. Phys.* **1986**, *84*, 4524.
(25) Ziegler, T. *Chem. Rev.* **1991**, *29*, 55 and references therein.
(26) Morokuma, K. *J. Chem. Phys.* **1971**, *55*, 1236.
(27) Ziegler, T.; Rauk, A. *Inorg. Chem.* **1979**, *18*, 1558.
(28) Ziegler, T.; Rauk, A. *Inorg. Chem.* **1979**, *18*, 1755.
(29) Fujimoto, H.; Osamura, J.; Minato, T. *J. Am. Chem. Soc.* **1978**, *100*, 2954.
(30) Kitaura, K.; Morokuma, K. *Int. J. Quantum Chem.* **1976**, *10*, 325.
(31) Van den Hoek, P. J.; Kleyn, A. W.; Baerends, E. J. *Comments At. Mol. Phys.* **1989**, *23*, 93.
(32) Ziegler, T.; Rauk, A. *Theor. Chim. Acta* **1977**, *46*, 1.
(33) Bickelhaupt, F. M.; Nibbering, N. N.; van Wezenbeek, E. M.; Baerends, E. J. *J. Phys. Chem.* **1992**, *96*, 4864.
(34) Williams, G. A.; Figgis, B. N.; Mason, R.; Mason, S. A.; Fielding, P. E. *J. Chem. Soc., Dalton Trans.* **1980**, 1688.
(35) Brown, C. J. *J. Chem. Soc. A* **1968**, 2488.
(36) Robertson, J. M. *J. Chem. Soc.* **1936**, 1195.
(37) Schramm, C. J.; Scaringe, R. P.; Stojakovic, D. R.; Ibers, J. A.; Marks, T. J. *J. Am. Chem. Soc.* **1980**, *102*, 6702–6713.
(38) Fischer, M. S.; Templeton, D. H.; Zalkin, A.; Calvin, M. *J. Am. Chem. Soc.* **1971**, *93*, 2622.
(39) Hoard, J. L.; Hamor, M. J.; Hamor, T. A. *J. Am. Chem. Soc.* **1963**, *85*, 2334.
(40) Fleischer, E. B.; Miller, C. K.; Webb, L. E. *J. Am. Chem. Soc.* **1964**, *86*, 2342.

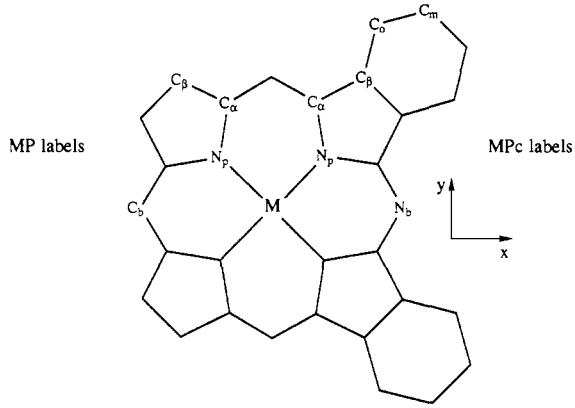

Figure 1. Atom labeling scheme for metal phthalocyanine, MPc (right side) and porphyrin, MP (left side).

Table 1. Distance (Å) of the Metal Center from the Pyrrolic Nitrogens for MPc's (M = Mg, Co, Ni, Cu) and NiP and Optimized N_p–H Distances for Metal-Free Phthalocyanine, H_2Pc, and Metal-Free Porphyrin, H_2P

	MgPc							
	D_{4h}	C_{4v}	CoPc	NiPc	CuPc	NiP	H_2Pc	H_2P
M–N_p	1.98	2.04	1.92	1.89	1.93	1.96		
N_p–H							1.02	0.98

As concerns the free-base phthalocyanine and porphyrin, the correct description of the location of the protons is a matter of some controversy[41-46] and two geometrical configurations (D_{2h} symmetry) have been proposed as the most likely candidates: (i) bonded, with H's attached to two opposing nitrogens, and (ii) bridged, with H's shared between adjacent nitrogens. The most recent experimental data for phthalocyanine[47] and related porphine molecules[48] provide, however, evidence for a bonded structure. With the aim to contribute to the resolution of this problem, we treated H_2Pc and H_2P in both geometrical configurations. The coordinates of Pc and P rings have been derived from experiment,[47a,48] with appropriate averaging of bond angles and bond lengths to preserve the carbon–nitrogen skeleton in D_{4h} symmetry, while the N_p–H distance has been optimized. Our calculations clearly favor a bonded structure for both molecules. We find indeed that H_2Pc and H_2P in the bonded configuration are 142.1 and 240.9 kJ mol^{-1} lower in energy than in the bridged one. As shown in Table 1, wherein are collected some relevant bond parameters used in the calculations reported in this paper, the H_2Pc and H_2P optimized N_p-H distances are 1.02 and 0.98 Å, respectively, somewhat too long compared to 0.94 and 0.86 Å of the experiments.[47a,48] This discrepancy is largely due to the fact that the carbon–nitrogen backbone was kept fixed during the optimization. The coordinate system as well as the labeling of the nonequivalent atomic centers in the ring is shown in Figure 1.

3. MPc Ground-State Electronic Structure

(a) Level Schemes and Population Analyses. It is useful to compare level schemes of related molecules, as differences and similarities in bonding mechanisms are often clearly displayed by the relative position of similar levels. We show in Figure 2 the one-electron levels obtained by spin restricted calculations for the MPc series (M = Mg, Co, Ni, Cu), together with the levels of the bare macrocycle, the phthalocyanine dianion, Pc^{2-}.

Table 2. Percent Contribution of Pc and M Fragments to Selected Orbitals (Based on Mulliken Population Analysis per MO) of Metallophthalocyanines with M = Co, Ni, Cu, where only the Main Contributions to Each Orbital Have Been Given

		ϵ (eV)	M	Pc
$7e_g$	CoPc	−4.16	5.3 (d_π)	94.7 ($6e_g$)
	NiPc	−4.17	4.9 (d_π)	95.1 ($6e_g$)
	CuPc	−4.12	1.5 (d_π)	98.5 ($6e_g$)
$11b_{2g}$	CoPc	−3.61	61.7 (d_{xy})	38.3 ($10b_{2g}$ – N_p lone pair)
	NiPc	−4.24	55.4 (d_{xy})	44.6 ($10b_{2g}$ – N_p lone pair)
	CuPc	−4.88	49.0 (d_{xy})	51.0 ($10b_{2g}$ – N_p lone pair)
$2a_{1u}$	CoPc	−5.64	0.0	100.0 ($2a_{1u}$)
	NiPc	−5.73	0.0	100.0 ($2a_{1u}$)
	CuPc	−5.67	0.0	100.0 ($2a_{1u}$)
$9b_{1g}$	CoPc	−6.23	42.6 ($d_{x^2-y^2}$)	57.4 ($8b_{1g}$ – N_b lone pair)
	NiPc	−6.70	19.1 ($d_{x^2-y^2}$)	80.9 ($8b_{1g}$ – N_b lone pair)
	CuPc	−6.53	4.0 ($d_{x^2-y^2}$)	95.6 ($8b_{1g}$ – N_b lone pair)
$6e_g$	CoPc	−6.09	59.1 (d_π)	40.9 ($5e_g$)
	NiPc	−6.31	59.6 (d_π)	40.4 ($5e_g$)
	CuPc	−6.71	15.3 (d_π)	84.7 ($5e_g$)
$4a_{2u}$	CoPc	−7.40	2.5 (p_z)	97.5 ($4a_{2u}$)
	NiPc	−7.63	2.2 (p_z)	97.8 ($4a_{2u}$)
	CuPc	−7.27	2.6 (p_z)	97.4 ($4a_{2u}$)
$13a_{1g}$	CoPc	−6.53	95.9 (d_{z^2}, 4s)	4.1 ($11a_{1g}$)
	NiPc	−6.24	96.6 (d_{z^2}, 4s)	3.4 ($11a_{1g}$)
	CuPc	−7.60	38.2 (d_{z^2})	61.8 ($10a_{1g}$, $11a_{1g}$)
$12a_{1g}$	CoPc	−7.69	0.0	100.0 ($10a_{1g}$, $11a_{1g}$)
	NiPc	−7.89	0.0	100.0 ($10a_{1g}$, $11a_{1g}$)
	CuPc	−7.64	56.9 (d_{z^2}, 4s)	43.7 ($10a_{1g}$)
$4e_g$	CoPc	−7.49	26.2 (d_π)	73.8 ($5e_g$, $3e_g$)
	NiPc	−7.61	26.0 (d_π)	74.0 ($5e_g$, $3e_g$)
	CuPc	−8.04	60.0 (d_π)	40.0 ($3e_g$)
$8b_{1g}$	CoPc	−7.22	53.3 ($d_{x^2-y^2}$)	46.7 ($8b_{1g}$)
	NiPc	−7.93	80.0 ($d_{x^2-y^2}$)	20.0 ($8b_{1g}$)
	CuPc	−8.48	91.8 ($d_{x^2-y^2}$)	8.2 ($8b_{1g}$)
$3e_g$	CoPc	−8.93	5.7 (d_π)	94.3 ($3e_g$, $5e_g$)
	NiPc	−9.14	6.2 (d_π)	93.8 ($3e_g$, $5e_g$)
	CuPc	−9.00	19.3 (d_π)	80.7 ($3e_g$, $5e_g$)
$16e_u$	CoPc	−9.72	5.9 (p_σ)	94.1 ($18e_u$, $15e_u$)
	NiPc	−9.98	5.6 (p_σ)	94.4 ($18e_u$)
	CuPc	−9.54	4.8 (p_σ)	95.2 ($18e_u$, $15e_u$)
$9b_{2g}$	CoPc	−10.99	21.1 (d_{xy})	78.9 ($8b_{2g}$, $10b_{2g}$)
	NiPc	−10.71	21.0 (d_{xy})	79.1 ($8b_{2g}$, $10b_{2g}$)
	CuPc	−10.40	26.6 (d_{xy})	73.4 ($8b_{2g}$, $10b_{2g}$)

The Pc^{2-} levels have been rigidly shifted by 6.3 eV to lower energies in order to bring the $2a_{1u}$ levels into correspondence. This allows us to use the Pc^{2-} levels as a reference to evaluate the perturbation effects induced by different metals. In Figure 2 we omit the orbital energies for nonplanar C_{4v} Mg as the level scheme is the same as for planar except that the empty $7a_{2u}$ (a_1 in C_{4v}) orbital, which lies well above the empty $6e_g(\pi^*)$ and is not shown in the diagram, is considerably (0.7 eV) stabilized. As the metal moves out of the plane the $7a_{2u}$ (49% $3p_z$) loses part of its $3p_z$ character and acquires a large 3s percentage: the composition of this orbital in the planar geometry is 49% Mg ($3p_z$) and 51% Pc–π and becomes 65% Mg (3s), 16% Mg ($3p_z$), 2.6% Mg ($3d_z2$), and 16.4% Pc–π in the nonplanar geometry. The ground states of MgPc, CoPc, NiPc, and CuPc are $^1A_{1g}$, $^2A_{1g}$, $^1A_{1g}$, and $^2B_{2g}$, respectively, with occupation of the one-electron levels as indicated in Figure 2 (the open shell systems, CoPc and CuPc, have also been calculated spin-unrestricted, see Figure 3). It is clear that the highest *fully* occupied molecular orbital is invariably the $2a_{1u}$ which is a pure macrocycle orbital and lies in all systems at the same energy.

For a discussion of the trends in the one-electron energies it is instructive to look at the composition of the individual orbitals. In Table 2 the composition of the most important orbitals is given in terms of metal and Pc orbitals, and Table 3 displays the Mulliken populations of these fragment orbitals. We feel these populations

(41) Schäffer, A. M.; Gouterman, M. T. *Theor. Chim. Acta* **1972**, *25*, 62.
(42) Gouterman, M.; Wagniere, G. H.; Snyder, L. L. *J. Mol. Spectrosc.* **1963**, *11*, 103.
(43) Henriksson, A.; Roos, B.; Sundbom, M. *Theor. Chim. Acta* **1972**, *27*, 303.
(44) Chen, I.; Abkowitz, M. *J. Chem. Phys.* **1969**, *50*, 2237.
(45) Chen, I. *Mol. Spectrosc.* **1967**, *23*, 131; *J. Chem. Phys.* **1969**, *51*, 3241.
(46) Sukigara, M.; Nelson, R. C. *Mol. Phys.* **1969**, *17*, 387.
(47) Niwa, I.; Lobayashi, H.; Tsuchida, T. (a) *J. Chem. Phys.* **1974**, *60*, 799; (b) *Inorg. Chem.* **1974**, *13*, 2891.
(48) (a) Chen, B. M. L.; Tulinsky, A. *J. Am. Chem. Soc.* **1972**, *94*, 414. (b) Wehrle, B.; Linbach, H.-H.; Köcher, M.; Ermer, O.; Vogel, E. *Angew. Chem., Int. Ed. Engl.* **1987**, *26*, 934. (c) Frydman, L.; Olivieri, A. C.; Diaz, L. E.; Frydman, B.; Morin, F. G.; Mayne, C. L.; Grant, D. M.; Adler, A. D. *J. Am. Chem. Soc.* **1988**, *110*, 336.

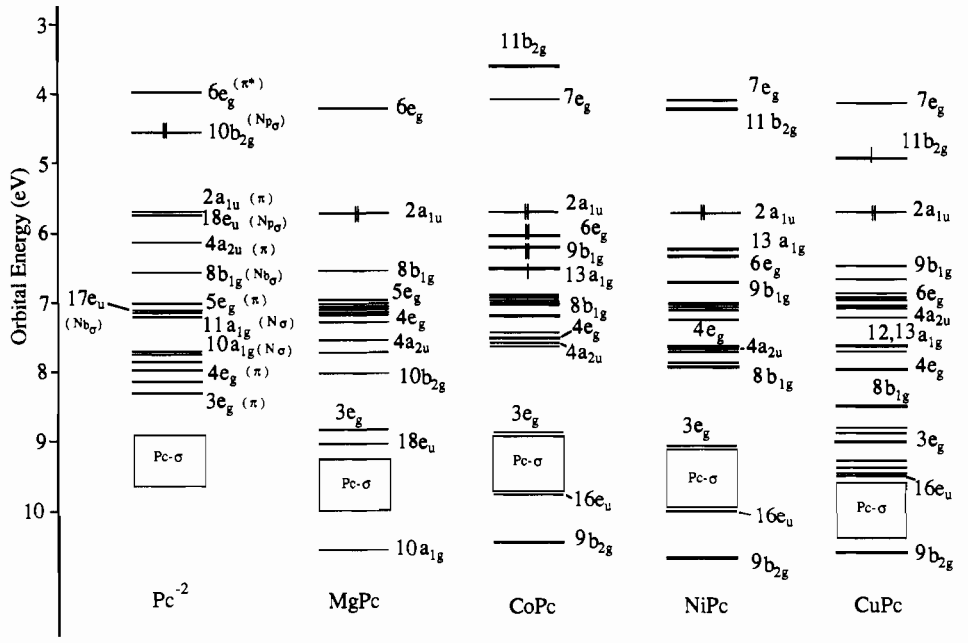

Figure 2. Energy level scheme for Pc^{2-} and MPc's (M = Mg, Co, Ni, Cu). The heavy lines indicate the orbitals which are predominantly of metal character. Double occupancy is indicated for the HOMO only ($10b_{2g}$ and $2a_{1u}$, respectively). All lower lying orbitals are also doubly occupied, except for $13a_{1g}$ of CoPc (singly occupied).

Table 3. Mulliken Gross Population of SCF Orbitals of Pc and M Fragments in Metallophthalocyanines with M = Mg, Co, Ni, and Cu, Where All Virtual Orbitals of a Given Symmetry (Other Than the One Given Explicitly) Are Collectively Denoted by a Prefix "*n*"

Γ			Mg (D_{4h})	Mg (C_{4v})	Co	Ni	Cu
A_{1g}	M	4s	0.2720 (3s)	0.2310 (3s)	0.3255	0.3941	0.4585
		$3d_{z^2}$	0.0190	0.0131	1.0253	1.9016	1.9467
		nd_{z^2}			0.0135	0.0141	0.0000
	Pc	$10a_{1g}$	1.9699	1.9723	1.8964	1.8538	1.8982
		$11a_{1g}$	1.7434	1.7596	1.7451	1.8244	1.6854
		na_{1g}	0.0082	0.0090	0.0163	0.0043	0.0134
B_{1g}	M	$3d_{x^2-y^2}$	0.0116	0.0097	1.9510	1.9597	1.9759
		$nd_{x^2-y^2}$			0.0091	0.0112	0.0042
	Pc	$8b_{1g}$	1.9944	1.9949	1.9974	1.9969	1.9977
		nb_{1g}	0.0013	0.0084	0.0448	0.0371	0.0260
B_{2g}	M	$3d_{xy}$	0.1926	0.1517	0.8024	0.9041	1.5341
		nd_{xy}			0.0744	0.0740	0.0638
	Pc	$10b_{2g}$	1.8160	1.8504	1.1192	1.0168	1.3978
		nb_{2g}	0.0023	0.0113	0.0146	0.0023	0.0094
E_g	M	$3d_\pi$	0.0216	0.0482	3.7208	3.7480	3.9150
		nd_π			0.0156	0.0155	0.0000
	Pc	$5e_g$	3.8130	3.8254	3.8932	3.8900	3.8704
		$6e_g$	0.1162	0.1110	0.2434	0.2310	0.1356
		ne_g	0.0632	0.0244	0.1422	0.1404	0.0836
A_{2u}	M	$3p_z$	1.9999 ($2p_z$)	1.9997 ($2p_z$)	2.0000	1.9999	1.9998
		np_z	0.0467	0.0514	0.0032	0.0306	0.0340
	Pc	$4a_{2u}$	1.9214	1.9108	1.9119	1.9231	1.9147
		na_{2u}	0.0350	0.0353	0.0491	0.0443	0.0398
E_u	M	$3p_\sigma$	4.0018 ($2p_\sigma$)	3.9988 ($2p_\sigma$)	3.9966	3.9954	3.9964
		np_σ	0.3942	0.3935	0.2656	0.2846	0.3018
	Pc	$18e_u$	3.6408	3.6196	3.7180	3.7064	3.6660
		ne_u	0.0334	0.0346	0.0261	0.0036	0.0241

Gross Charges

	Mg (D_{4h})	Mg (C_{4v})	Co	Ni	Cu
M	+1.0709	+1.0948	+0.7952	+0.7016	+0.8029
N_p	−0.7573	−0.7312	−0.6888	−0.6952	−0.6995
N_b	−0.4516	−0.4531	−0.4507	−0.4410	−0.4499
C_α	+0.4002	+0.3875	+0.3961	+0.4005	+0.4049
C_β	−0.0386	−0.0387	−0.0202	−0.0275	−0.0213
C_o	−0.2330	−0.2339	−0.2643	−0.2411	−0.2656
C_m	−0.2693	−0.2702	−0.2930	−0.2644	−0.2951

to be more informative than the usual populations of primitive basis functions, particularly when one is interested in describing metal–ligand bonding. From Tables 2 and 3 the metal–Pc interactions can be easily traced out.

In-Plane Interactions. The in-plane Pc orbitals that play a role consist of symmetry combinations of N_p and N_b lone pairs. In D_{4h} symmetry the four N_p lone pair combinations transform as b_{2g}, e_u, a_{1g} and the four N_b lone pair combinations as b_{1g}, e_u, a_{1g}. The related Pc^{2-} orbitals can be recognized in Figure 2 as the $10b_{2g}$, $18e_u$, and $11a_{1g}$ N_p orbitals, and the $8b_{1g}$, $17e_u$, and $10a_{1g}$ N_b orbitals (the $10a_{1g}$ and $11a_{1g}$ orbitals have mixed N_b/N_p character). In Pc^{2-} the N_p lone pairs are relatively high lying due to the negative charge. As shown in Table 3, even in the MPc complexes where a large donation takes place from the N_p lone pairs to the metal, the charge on N_p lone pairs is more negative than on N_b lone pairs (about 0.24 electron). We will consider the interactions in the various irreducible representations in turn.

Concerning the B_{1g} symmetry we observe that of all the nitrogen lone pair orbitals the Pc–$10b_{2g}$ N_p lone pair orbital is by far the highest; it is the HOMO of the dianion. It mixes in a strong σ interaction with the favorably oriented lobes of the empty d_{xy} metal orbital to form the $11b_{2g}$ and $9b_{2g}$ MO's of the complexes. The $11b_{2g}$ orbital, which is empty except in CuPc where it gets occupied with one electron, is an antibonding M–N_p state composed of metal $3d_{xy}$ and Pc–$10b_{2g}$ in almost equal amount. Its bonding counterpart, the $9b_{2g}$, is much lower in energy, indicating the strength of the σ interaction. The bonding, respectively antibonding nature of these orbitals is clearly displayed in the plots of Figure 4. The energy gap between the $11b_{2g}$ and its bonding partner is 6.87, 6.47, and 5.53 eV for CoPc, NiPc, and CuPc, respectively, indicating a weaker M–N_p interaction in CuPc. This is reasonable in view of the smaller M–N_p overlap due to the contraction going from Co to Cu $3d_{xy}$ and at the same time the larger M–N_p bond length in CuPc (1.93 Å in CuPc vs 1.92 Å in CoPc and 1.89 Å in NiPc). The populations given in Table 3 confirm the strong interaction in B_{2g} symmetry. They show that the largest charge transfers occur in this symmetry: 0.87, 0.97, and 0.60 electrons are donated to cobalt, nickel, and copper d_{xy}, respectively, from the Pc–$10b_{2g}$ N_p lone pair. In particular for Co and Ni the situation in this symmetry is actually close to a homopolar electron pair bond between metal and ring.

In B_{1g} symmetry there is mainly repulsive interaction. The Pc–$8b_{1g}$ is mostly a N_b lone pair orbital, but also contains some N_p in-plane p_π that makes it suitable for in-plane π interaction with the occupied $d_{x^2-y^2}$. This interaction occurs in the $8b_{1g}$ and

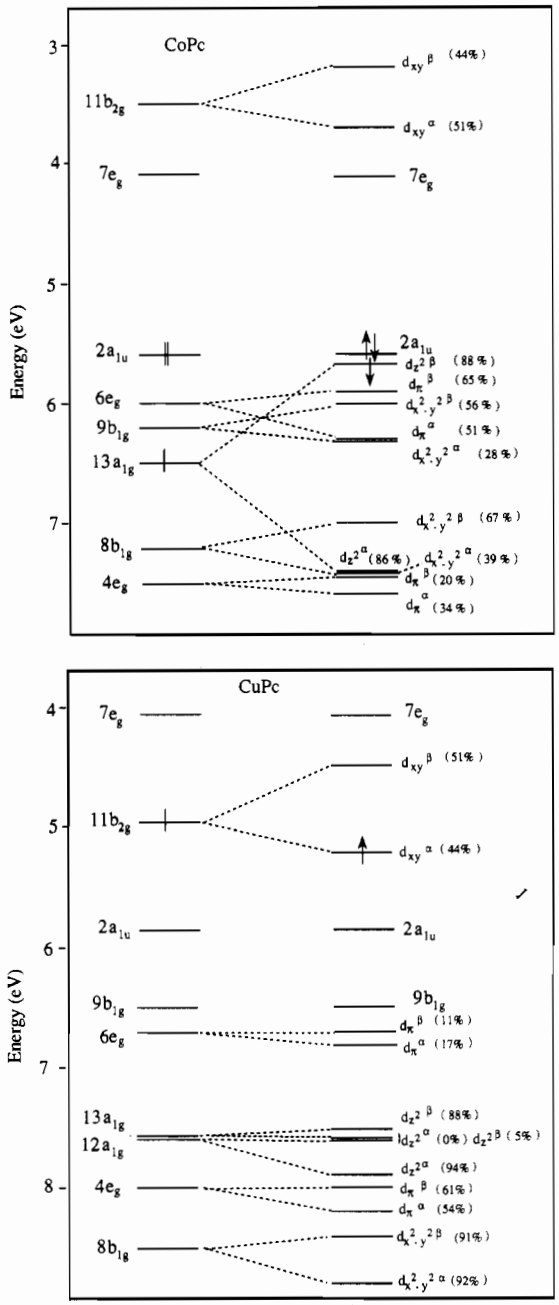

Figure 3. Orbital energies from spin restricted (right side) and spin unrestricted (left side) calculations: (a, top) CoPc; (b, bottom) CuPc. In the spin unrestricted calculations results, the small splittings of phthalocyanine α and β orbitals are not shown. The orbital population is also given for spin-up and spin-down components.

$9b_{1g}$ MO's, metal–N_p π bonding and antibonding respectively, as inferred by the plots of Figure 5. As the plots clearly show, the bridging nitrogen lone pairs, although strongly contributing to $8b_{1g}$ and $9b_{1g}$, have the largest amplitude away from the inside of the ring and are thus not suitable for σ interaction with the $d_{x^2-y^2}$ orbital of the central atom. The mixing percentage of $d_{x^2-y^2}$ with the Pc–$8b_{1g}$ decreases along our series: while in CoPc it is involved approximately to the same extent in $8b_{1g}$ (53%) and $9b_{1g}$ (43%), we find the $d_{x^2-y^2}$ almost purely in the $8b_{1g}$ MO of NiPc and CuPc (80% and 92%, respectively). This trend is the result of two effects: (i) decrease of the overlap between the $d_{x^2-y^2}$ and the Pc–$8b_{1g}$, as in the case of the d_{xy} discussed before; (ii) energy mismatch of the interacting orbitals, due to the downward energy shift of the d orbitals on going from cobalt to copper. From the populations given for the B_{1g} symmetry in Table 3 it is immediately apparent that the $d_{x^2-y^2}$ mixes only slightly with virtual Pc orbitals of this symmetry which lie at too high an energy. The π in-plane

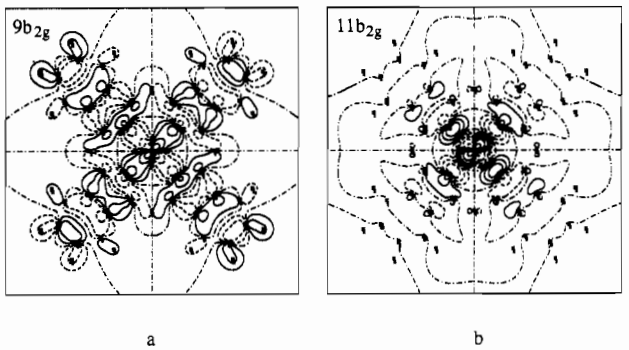

Figure 4. Contour plots of (a) MPc (M = Co) $9b_{2g}$ bonding and (b) $11b_{2g}$ antibonding orbitals in the molecular plane (the orientation of the molecule is as in Figure 1a). Contour values are 0.0, ±0.02, ±0.05, ±0.1, ±0.2, and ±0.5 $[e/bohr^3]^{1/2}$.

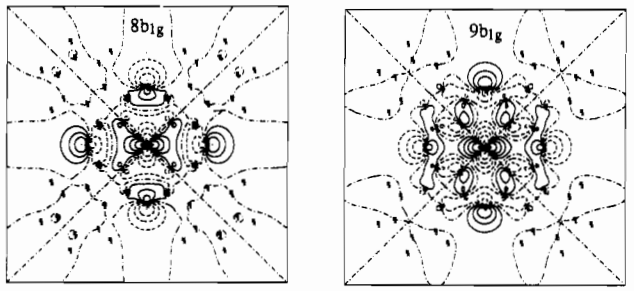

Figure 5. Contour plots of MPc (M = Co) (a) $8b_{1g}$ bonding and (b) $9b_{1g}$ antibonding. See caption to figure 4.

interaction is therefore primarily a two-orbital, four-electron destabilizing interaction between the occupied $d_{x^2-y^2}$ metal and the occupied Pc $8b_{1g}$ orbital. Because of the lack of occupied–virtual interaction one may not expect a significant B_{1g} contribution to the metal–macrocycle bond in any compound of the series, a point to which we will return below.

As concerns the Pc lone pair orbitals of E_u symmetry, the low-lying Pc $17e_u$ is not suitable for interaction with the metal, being a N_b lone pair orbital, while the Pc $18e_u$, which is located on pyrrolic nitrogens, combines with $4p_\sigma$ orbitals to form the MPc $16e_u$. Although the mixing of the $4p_\sigma$ is quite small, less than 6%, the $16e_u$ is considerably lower than its parent $18e_u$ in Pc^{2-}, indicating a significant contribution of $4p_\sigma$ to the metal–Pc bond. According to the fragment orbital populations in E_u symmetry, considerable σ donation does take place from Pc–$18e_u$ into the virtual np_σ orbitals (mainly $4p_\sigma$), the population of which uniformly increases along the series.

M–Pc in-plane interaction also occurs in A_{1g} symmetry. The considerable 4s population is mainly coming from Pc σ orbitals ($10a_{1g}$,$11a_{1g}$). The low lying Pc-$11a_{1g}$ and Pc-$10a_{1g}$ orbitals are composed of N_p and N_b lone pair combinations; the former however contains a larger percentage of N_p lone pairs (61% N_p, 19% N_b) that makes it well adapted to interact with the 4s and the ring of the d_{z^2}. The Pc–$11a_{1g}$ accordingly loses more charge than the Pc–$10a_{1g}$. In nickel and copper the 4s orbital also picks up some charge from $3d_{z^2}$. This implies that the 4s populations do not faithfully represent the amount of charge coming out of Pc-σ orbitals, which is actually 0.34, 0.32, and 0.40 electron in Co, Ni, and Cu respectively. The $12a_{1g}$ and $13a_{1g}$ MPc orbitals, where these interactions occur, exhibit the lowering of the metal states towards Cu. In CoPc and NiPc the $13a_{1g}$ is mainly a pure metal orbital, largely (87%) d_{z^2} with some (9%) 4s character and a small admixture of Pc–$11a_{1g}$. In CuPc the d_{z^2} character gets divided over $13a_{1g}$ and $12a_{1g}$ and the 4s character occurs in $12a_{1g}$ rather than in $13a_{1g}$. The $13a_{1g}$ whose energy is very sensitive to the nature of the metal (see Figure 2), is "anomalously" low

in CoPc. This may be artificial, being related to its single occupancy in the CoPc ground state.

Out-of-Plane Interactions. We now turn to the *out-of-plane* (π) interactions, which only involve a_{2u} and e_g type orbitals. In E_g symmetry the interaction is primarily between the occupied metal d_π and occupied Pc π orbitals, mostly $5e_g$ (owing to a sizable (28%) N_p p_π character) and $3e_g$. However, the spacing of the resulting π bonding/antibonding pair $4e_g/6e_g$ is much smaller than that of the σ bonding/antibonding pair $11b_{2g}/9b_{2g}$. In the $4e_g/6e_g$ pair the metal contribution in the $6e_g$ decreases on going from CoPc to CuPc and increases in the $4e_g$. In CuPc the $4e_g$ is largely metallic (60%), and also a sizable (19%) metal percentage is found in the low lying $3e_g$ MO. The downward shift of the occupied metal states when going from CoPc to CuPc is clearly distinguishable in the level scheme (Figure 2), but it is not uniform. It is noteworthy that the mixings that occur in e_g type orbitals mainly involve occupied Pc-π orbitals ($5e_g$ and $3e_g$), the participation of the lowest lying π virtual orbital, i.e. Pc–$6e_g$, being small but not negligible. The corresponding π back-donation of the filled d_π into the empty Pc–$6e_g$ amounts to 0.26 and 0.24 electron (Table 3) for cobalt and nickel. The charge transfer decreases along the series, as expected from the downward shift of the metal states on going from Co to Cu that increases the energy gap between the filled d_π and the empty Pc-π^* orbitals. The decrease is not uniform, however, the copper loses in fact less than 0.1 electron. In E_g symmetry there is also a clearly distinguishable polarization of the ligand. We note in fact that the empty Pc-π^* orbitals of E_g symmetry acquire in Co, Ni, and Cu charges of 0.3856, 0.3714, and 0.2192 electron, respectively, of which 0.2636, 0.2675, and 0.085 electron come out of d_π orbitals; the rest (0.1220, 0.1039, and 0.1342; in copper this is more than 60%) come from the occupied Pc-π orbitals.

In A_{2u} symmetry finally, the contribution of $4p_z$ to the π bond is almost negligible as expected. According to Table 2, the metal $4p_z$ mixes slightly with the Pc–$4a_{2u}$, which is composed of N_p (54%) and N_b (46%) p_π orbitals, to form the $4a_{2u}$ MO. This interaction, although not very effective, owing to the poor overlap between these orbitals, nevertheless stabilizes the $4a_{2u}$ in the complexes. The resulting $4p_z$ population (Table 3) is quite small, the charge transfer within the macrocycle orbitals (polarization) leading to even larger populations of the virtual Pc orbitals.

Mg versus Transition Metals. Comparing MgPc to transition metal phthalocyanines, we note that the alkaline earth complex has much in common with its transition metal analogues. The Mg 3s acts like TM 4s and in fact it mixes significantly (11%) with the Pc–$11a_{1g}$ orbital, which is now unable to interact with the high lying d_{z^2}. The resulting $10a_{1g}$ MO is considerably stabilized as the level scheme of Figure 2 shows. As consequence of this mixing, 0.27 electron is donated to the 3s from Pc-σ orbitals, mainly the Pc–$11a_{1g}$ (see Table 3). The lower population of 3s compared to 4s simply reflects the fact that the 3s mixes very little with deeper lying Pc-σ orbitals of A_{1g} symmetry such as Pc–$10a_{1g}$. The d_{z^2}, in accordance with the small percentage (1%) in which it mixes into the Pc–$11a_{1g}$ orbital, receives only 0.02 electron.

The Mg–$3p_{\sigma,z}$ orbitals also act like the TM $4p_{\sigma,z}$. The Mg–$3p_\sigma$ mixes to some extent (6%) with the Pc–$18e_u$ N_p lone pair, leading to stabilization of the $18e_u$ MO. The $3p_\sigma$ populations found in the E_u symmetry are considerably larger than the $4p_\sigma$ populations of transition metal phthalocyanines. Analogous to the $4p_z$, the Mg–$3p_z$ slightly mixes with the Pc–$4a_{2u}$ that is accordingly stabilized, although much less than the $18e_u$.

The Mg–3d orbitals, vacant in the ground state of the atom, have a very different role in the bond compared to TM 3d. The interaction between the $3d_{xy}$ and the Pc–$10b_{2g}$ N_p lone pair, which in TM phthalocyanines turns out to be the most important one, still occurs in MgPc, but is much weaker. The Mg $3d_{xy}$ in fact mixes little (11%) with the Pc $10b_{2g}$ to form the $10b_{2g}$ orbital of the complex. The stabilization of this orbital, Mg–N_p bonding in character, is clearly visible in the level scheme of Figure 2, but certainly is not comparable to the stabilization of the $9b_{2g}$ in the TM phthalocyanines. Actually, the Mgd_{xy} acquires only a charge of 0.2 electron, which is much less than the 0.87, 0.97 and 0.60 electron of Co, Ni, Cu d_{xy}.

No π in-plane interaction is found in MgPc where the $8b_{1g}$ remains a pure ligand orbital (its energy is the same as in Pc^{2-}). The $3d_{x^2-y^2}$ orbital is thus not involved at all in the bonding, as inferred also from its negligible charge (0.012).

The d_π orbitals also mix very little (1%) with the Pc–$5e_g$ occupied orbital, acquiring only 0.022 electron. In E_g symmetry we again find polarization of the macrocycle, which is even larger than with TM's. As we will see below, this polarization accounts for a large energy contribution in this symmetry. When comparing the nonplanar C_{4v} MgPc to the planar D_{4h}, we see that the populations of the fragment orbitals do not differ substantially (cf. Table 3), indicating that the displacement of Mg out of the plane has very little effect on the metal–macrocycle interactions.

Spin Unrestricted Calculations. The spin unrestricted molecular orbital energy diagrams shown in parts a and b of Figure 3 for the open shell systems, CoPc and CuPc, respectively, are representative of a general pattern in organometallic compounds. The highly delocalized ligand π orbitals (e.g. $2a_{1u}$, $7e_g$) see little exchange effect and the splitting between spin-up and spin-down is very small. By contrast, the molecular orbitals that are largely localized on the metal have sizable splitting, which is larger in cobalt where the spin density is completely located on the metal. The orbital shifts are also accompanied by significant changes of the amount of ligand mixing in the molecular orbital, as shown in Figure 3 where we see, for instance, that the lower-lying spin-up d_π orbitals mix more favorably with the Pc-π. The cobalt $6e_g\beta$ orbital has 65% d_π character, while $6e_g\alpha$ has 51%, indicating a slightly more covalent interaction with the ligand for α spin. An analogous behaviour is shown by the $4e_g$ copper orbital. The utility of spin unrestricted calculations to correctly interpret the differential up and down spin density measured in paramagnetic phthalocyanine complexes has been recently emphasized by Reynolds et al.[3] We will refer to these spin-unrestricted results when discussing the assignment of the metal-dependent photoelectron spectral features.

(b) Differences Pc/P. Phthalocyanine can be regarded as a derivative of porphyrin, where the aromatic system has been enlarged by the condensation of four benzene rings and the methine bridges have been substituted by aza bridges. The phthalocyanine framework is rather rigid and, compared to porphyrin, has a smaller hole size (the distance between the N_p atoms and the center of the molecule). In Pc^{2-} complexes the hole size is in fact at least 0.05 Å smaller than in P^{2-} complexes. This is due to the contraction of the azamethine bridge angle, which in turn is probably caused by steric requirements of the lone pair electrons on the azamethine nitrogen atoms.[49] The structural and electronic differences between Pc and P rings are expected to affect the metal–ring bond. We will address this issue starting from the analysis of the electronic structure of phthalocyanine and porphyrin ligands. In Figure 6 are shown the energy levels of the porphyrin dianion, P^{2-}. As in the case of the phthalocyanine dianion, the P^{2-} levels have been rigidly shifted to lower energies (by 7.3 eV), so as to bring the $1a_{1u}$ levels of the dianion and of the nickel porphyrin into correspondence. When comparing the one-electron level schemes of Pc^{2-} and P^{2-} (Figure 2 with respect to Figure 6) it is immediately apparent that in P^{2-} those orbitals are lacking that in Pc^{2-} have been identified as mainly N_b lone pair. Among these the Pc–$8b_{1g}$ is worth noting. As has already been stressed, this orbital is mostly N_b lone pair in character but also contains some in-plane N_p p_π that makes it suitable for π

(49) Hoard, J. L. "Porphyrins and Metalloporphyrins"; K. M. Smith, Ed., American Elsevier: New York, 1978; p 321.

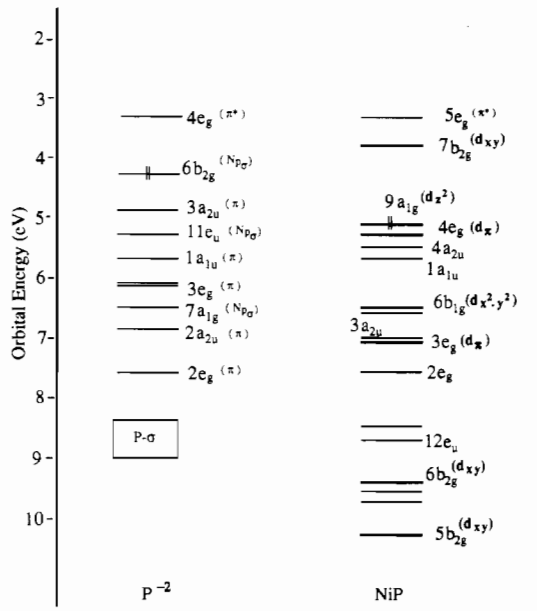

Figure 6. Energy level scheme for P^{2-} and NiP. The heavy lines indicate the orbitals which are predominantly of metal character. Double occupancy is indicated for the HOMO only ($6b_{2g}$ and $9a_{1g}$). All lower lying orbitals are also doubly occupied.

interaction with the $d_{x^2-y^2}$. In P^{2-} it still contains some amount of N_p p_π, but since it changes character, it is downward shifted, so it will no longer be able to interact repulsively with the occupied $d_{x^2-y^2}$ metal orbital. As concerns the N_p lone pair based orbitals ($6b_{2g}$, $11e_u$, and $7a_{1g}$ in P^{2-}), they do not differ significantly in the two macrocycles, neither in composition nor in energy. The P–$6b_{2g}$, analogous to the Pc–$10b_{2g}$ N_p lone pair, is the highest occupied in-plane orbital and is the HOMO of the porphyrin dianion. The P–$11e_u$ and Pc–$18e_u$ are also very similar, both are largely located on pyrrolic nitrogens (80%) and for the rest on C_α and C_β. The last lone pair orbital, the P–$7a_{1g}$, only differs from Pc–$11a_{1g}$ in that in the former the contribution of N_b lone pairs is missing. Looking next at the π orbitals, the differences between Pc and P appear more striking. In fact, as clearly shown in the level schemes of Figures 2 and 6, the highest lying P-π orbitals, i.e. the $3a_{2u}$ and $1a_{1u}$, with a gap of 0.8 eV, have in Pc^{2-} their order reversed to yield $4a_{2u}$ 0.4 eV below $2a_{1u}$. Semiempirical CNDO-CI calculations[50] on Pc^{2-} and P^{2-} and the related TAP^{2-} (tetraazaporphyrin) and TBP^{2-} (tetrabenzoporphyrin) dianions also indicate a stabilization of the a_{2u} and a parallel destabilization of the a_{1u} on going from P^{2-} to Pc^{2-}. The result is however only a decrease of the energy gap between these orbitals, the a_{1u} being the HOMO in all of the investigated dianions.

The above detailed analysis of the electronic structure of Pc and P points out that the orbitals that are suitable for in-plane and out-of-plane interactions with the metal, except for the b_{1g}, are quite similar in the two macrocycles. Thus, the change of the ligand framework is not expected to alter substantially the metal–macrocycle interactions. However, because of the smaller hole size, the metal macrocycle bonding interactions may be enhanced in phthalocyanine complexes. This means that the coordination properties of the two macrocycles might differ in degree but not in kind, a point that we have investigated using the electronic structure of a prototype porphyrin, NiP.

Looking at the in-plane interactions first, as reflected in the orbital compositions for NiP of table 4, the d_{xy} is seen to be strongly mixed with the P–$6b_{2g}$ N_p lone pair orbital of the ring, suggesting that this is again the main bonding interaction. The larger hole size than in NiPc, however, results in a considerably smaller splitting of the bonding ($5b_{2g}$) and antibonding ($7b_{2g}$) combinations of these fragment orbitals, as shown in the level scheme of Figure 6. The $d_{x^2-y^2}$ is found almost purely in $6b_{1g}$, indicating that, for the reasons discussed above, no π in-plane interaction with the pyrrolic nitrogens occurs. As expected, in-plane interactions also occur in E_u and A_{1g} symmetries. The P–$12e_u$ N_p lone pair orbital mixes to some extent with the $4p_\sigma$ of the metal. The P–$7a_{1g}$ lone pair orbital has a slight antibonding mixing into the almost purely metal orbital $9a_{1g}$ (90% d_{z^2}), which is alleviated by 4s admixture (8%). Looking at the out-of-plane interactions, we note that the d_π is heavily mixed with the P–$3e_g$, largely $N_p p_z$ in character, in four-electron two-orbital destabilizing interactions. The resulting bonding ($3e_g$) and antibonding ($4e_g$) MO's are less homopolar than in NiPc due to some energy mismatch of the fragment orbitals. The π back-donation from d_π to the $4e_g$ and higher ne_g is smaller than in NiPc (see below). As in MPc's, the $4p_z$ of the metal slightly mixes with the P–$3a_{2u}$ to form the $4a_{2u}$ that is stabilized.

When comparing the Mulliken gross populations of NiPc and NiP, given in Tables 3 and 5 respectively, one notes that there are only minor differences in the charge transfers that occur during the bond formation. The larger hole size of the porphyrin ring causes however a slightly less effective charge transfer. The d_{xy} acquires 0.93 electron and 0.20 electron come out of d_π, to be compared with 0.98 and 0.27 electron, which are transferred in NiPc. A few other points are worth noting about the charge transfers in NiP. The population of higher lying ne_g orbitals is almost negligible, due to the fact that, unlike in phthalocyanines,

Table 4. Percentage Contribution of P and M Fragments to Lowest Unoccupied and Highest Occupied Orbitals (Based on Mulliken Population Analysis per MO) of NiP, where Only the Main Contributions to Each Orbital Has Been Given

	ϵ (eV)	Ni	P
$5e_g$	−3.31	4.3 (d_π)	95.7 ($4e_g$–π^*)
$7b_{2g}$	−3.78	56.7 (d_{xy})	43.3 ($6b_{2g}$–N_p lone pair)
$9a_{1g}$	−5.13	97.6 (d_{z^2}, 4s)	2.4 ($7a_{1g}$)
$4e_g$	−5.31	72.5 (d_π)	27.5 ($3e_g$)
$4a_{2u}$	−5.51	1.3 (p_z)	98.7 ($3a_{2u}$)
$1a_{1u}$	−5.67	0.0	100.0 ($1a_{1u}$)
$6b_{1g}$	−6.50	94.0 ($d_{x^2-y^2}$)	6.0 ($5b_{1g}$)
$2b_{1u}$	−6.58	0.0	100.0 ($2b_{1u}$)
$3a_{2u}$	−6.97	1.4 (p_z)	98.7 ($2a_{2u}$)
$3e_g$	−7.05	20.7 (d_π)	79.3 ($3e_g$)
$2e_g$	−7.50	0.0	100.0 ($2e_g$)
$1b_{2u}$	−8.53	0.0	100.0 ($1b_{2u}$)
$12e_u$	−8.69	5.7 (p_σ)	94.3 ($12e_u$–N_p lone pair)
$6b_{2g}$	−9.36	15.5 (d_{xy})	84.5 ($5b_{2g}$, $6b_{2g}$)
$11e_u$	−9.71	0.5 (p_σ)	95.5 ($10e_u$)
$5b_{1g}$	−9.96	3.3 ($d_{x^2-y^2}$)	96.7 ($5b_{1g}$)
$5b_{2g}$	−10.29	24.2 (d_{xy})	75.8 ($5b_{2g}$, $6b_{2g}$)

Table 5. Mulliken Gross Population of SCF Orbitals of P and Ni Fragments in NiP, Where All Virtual Orbitals of a Given Symmetry (Other Than the One Given Explicitly) Are Collectively Denoted by a Prefix "*n*"

A_{1g}	Ni	4s	0.4319	E_g	Ni	$3d_\pi$	3.7828
		$3d_{z^2}$	1.9073			nd_π	0.0154
		nd_{z^2}	0.0144				
	P	$6a_{1g}$	2.0006		P	$3e_g$	3.9336
		$7a_{1g}$	1.6436			$4e_g$	0.1834
		na_{1g}	0.0161			ne_g	0.0444
B_{1g}	Ni	$3d_{x^2-y^2}$	1.9586	A_{2u}	Ni	$3p_z$	2.0000
		$nd_{x^2-y^2}$	0.0103			np_z	0.0400
	P	$5b_{1g}$	1.9940		P	$3a_{2u}$	1.9285
		nb_{1g}	0.0399			na_{2u}	0.0290
B_{2g}	Ni	$3d_{xy}$	0.8576	E_u	Ni	$3p_\sigma$	3.9956
		nd_{xy}	0.0711			np_σ	0.3504
	P	$6b_{2g}$	1.0575		P	$11e_u$	3.6172
		nb_{2g}	0.0252			ne_u	0.0331

Gross Charges

Ni	N_p	C_b	C_α	C_β
+0.5917	−0.6327	−0.2864	+0.1986	−0.2863

(50) Lee, L. K.; Sabelli, N. H.; LeBreton, P. R. *J. Phys. Chem.* **1982**, *86*, 3926.

Table 6. Decomposition of the Bonding Energy for MPc's (M = Mg, Co, Ni, Cu) and NiP in Terms of M^{2+} and Pc^{2-} (P^{2-}) Ionic Fragments

	ΔE^0	$\Delta E_{A_{1g}}$	$\Delta E_{B_{1g}}$	$\Delta E_{B_{2g}}$	ΔE_{E_g}	$\Delta E_{A_{2u}}$	ΔE_{E_u}	ΔE_{nb}	ΔE_{oi}	$\Delta E_{oi} + \Delta E^0$
MgPc	−18.86	−1.20	−0.35	−0.80	−2.26	−0.76	−2.11	−1.29	−8.77	−27.63
CoPc[a]	−17.51	−2.62	−0.78	−5.81	−2.62	−0.96	−2.48	−1.73	−17.00	−34.51
NiPc	−18.05	−2.04	−0.75	−6.96	−2.61	−0.92	−2.61	−1.77	−17.66	−35.71
CuPc[b]	−18.30	−2.11	−0.67	−3.32	−2.58	−0.84	−2.51	−1.49	−13.52	−31.82
NiP	−21.74	−1.93	−0.73	−6.51	−1.69	−0.73	−2.75	−1.20	−15.54	−37.28

[a] Data from spin unrestricted calculations. [b] Data from unrestricted calculations. The open shell fragment method has been used (see ref 33).

there are no low-lying empty π^* orbitals. As we have already found in NiPc, the 4s population is quite large, and although it is mainly coming from P–$7a_{1g}$ orbital, the d_{z^2} also contributes. The $4p_\sigma$ AO's are, by virtue of the large population, clearly involved in the bonding, as in NiPc, but the $4p_z$ much less so.

In spite of similar metal–macrocycle interactions and hence similar orbital splittings, the level schemes of NiP and NiPc show some relevant differences, which are related to the particularities of the phthalocyanine and porphyrin rings discussed above. In NiP in fact the HOMO is the $9a_{1g}$ (d_{z^2}), which is a metal state, unlike in NiPc (and in other metallophthalocyanines as well) where the highest occupied orbital is invariably the $2a_{1u}$ (π) ligand orbital. This is the consequence of the destabilization of $2a_{1u}$ (π) orbital in phthalocyanine, induced by the benzene rings. The reversed order of $1a_{1u}$ and $3a_{2u}$ orbitals found in P^{2-} still holds in the nickel complex, but here, as shown in Figure 6, these orbitals, which correspond to the $1a_{1u}$ and $4a_{2u}$ in NiP, become almost degenerate owing to the stabilization of the $4a_{2u}$ by interaction with $4p_z$ of the metal. In phthalocyanine complexes the $2a_{1u}$ lies instead well above the $4a_{2u}$, and these two orbitals always straddle metal states and other ring orbitals.

(c) Metal–Macrocycle Bonding Energies. The charge rearrangements are a qualitative indication for the relative strengths of the metal-macrocycle interactions, but not a quantitative measure of the corresponding energies. Those are explicitly calculated according to the energy decomposition scheme discussed in section 2 and displayed in Table 6, for all considered MPc's (M = Mg, Co, Ni, Cu) and for our model porphyrin, NiP. In order to have clear and meaningful energy contributions in the individual irreducible representations, we promote the fragments to the ionic configurations Pc^{2-} (or P^{2-}) and M^{2+} [Co, $(d_{x^2-y^2})^2 (d_\pi)^4 (d_{z^2})^1 (d_{xy})^0 (4s)^0$; Ni, $(d_{x^2-y^2})^2 (d_\pi)^4 (d_{z^2})^2 (d_{xy})^0 (4s)^0$; Cu, $(d_{x^2-y^2})^2 (d_\pi)^4 (d_{z^2})^2 (d_{xy})^1 (4s)^0$; Mg, $(2p_\sigma)^4 (2p_z)^2 (3s)^0$]. It should be noted that our analysis, using valence states of the fragments, refers to the final situation, with the bonds formed. This change of configuration has the advantage that the Pauli repulsion due to 4s[6,54] (3s in the case of Mg) disappears. The Md_{xy} is emptied or partially emptied in the case of Cu and acts as acceptor orbital for electrons from the occupied Pc^{2-} or P^{2-} b_{2g} orbital.

Steric Interaction. As shown in the first column of Table 6, the steric interaction energy ΔE^0 is strongly attractive, due to the fact that the stabilizing contribution arising from the large attractive interaction between the charged fragments, ΔE_{elstat}, overcomes the positive (destabilizing) Pauli repulsion term, ΔE_{Pauli}. Looking first at phthalocyanine complexes, we note that the ΔE^0 term becomes more negative along the transition metal series, but it is largest in MgPc. Analysis of the contributions to the steric term (electrostatic interaction and Pauli repulsion) reveals that the electrostatic term behaves approximately as a function of the hole size, and accordingly (see Table 1) becomes more attractive (−24.49 to −28.40 to −28.96 to −29.66) in the series Mg–Cu–Co–Ni. The Pauli repulsion increases (+5.64 to +10.10 to +11.45 to +11.61) along the same series. In MgPc however it is about half of that found in the transition metal compounds, reflecting the considerably smaller number of closed shell electrons that can give rise to Pauli repulsion in MgPc (the 3s, 3p, and 3d shells are empty in Mg^{2+}) as compared to the transition metal phthalocyanines. The small ΔE_{Pauli} in MgPc causes the ΔE^0 in that compound to be the most negative in spite of the relatively small ΔE_{elstat}. Comparing now to NiP, we note that the steric interaction term is considerably more negative than in NiPc, the most appropriate phthalocyanine compound for comparison, indicating that the differences Pc/P are important. Both terms, ΔE_{Pauli} (8.93 eV) and ΔE_{elst} (−30.66 eV), change but the first much more due to the diminished number of fully occupied orbitals and to the larger hole size of the porphyrin macrocycle as well. The electrostatic interaction is more attractive than in NiPc, in spite of the larger hole size. This is still an effect of the macrocycle framework in the sense that it is due to the fact that the charge density on P^{2-} is higher than on Pc^{2-} where the charge can be delocalized on the macrocycle.

Polarization. As far as the orbital interaction energies are concerned, ΔE_{oi}, we would stress that as we are considering ionic interacting fragments (M^{2+} and Pc^{2-} or P^{2-}), it is expected that polarization is important. The decomposition in energy contributions belonging to different irreducible representations does not distinguish charge transfer and polarization. However, there are no metal orbitals that transform according to the A_{2g}, A_{1u}, B_{1u}, and B_{2u} symmetries and therefore the interaction energies in these "nonbonding" symmetries, which we collect in the term ΔE_{nb}, represent pure polarization, arising from interaction between occupied and virtual orbitals of Pc^{2-} and P^{2-} rings. The energetic effect of polarization (between 1.2 and 1.8 eV in these symmetries) is relatively small but not negligible. We will also identify polarization contributions in other symmetries.

In-Plane (σ) Bonding. From the data reported in Table 6 we note that the $\Delta E(B_{2g})$ term that accounts for σ-donation into the d_{xy} orbital is by far the largest one. Along the Co, Ni, and Cu series this term varies significantly, but not uniformly. In CuPc it is in fact strikingly smaller than in cobalt and nickel. This is simply due to the fact that in CuPc the antibonding $11b_{2g}$ orbital gets occupied by one electron; i.e., the σ interaction between Md_{xy} and Pc–$8b_{2g}$ orbitals is a two-orbital three-electron interaction. On going from CoPc to NiPc the $\Delta E(B_{2g})$ term increases by more than 1 eV, in line with the charge transfers observed in this symmetry. In NiP the $\Delta E(B_{2g})$ is slightly smaller than in NiPc (−6.51 vs −6.96), in agreement with the somewhat smaller charge transfer.

As expected, the contribution of $\Delta E(B_{1g})$ term is very small in all systems and decreases somewhat along the phthalocyanine series. We have already pointed out that admixing of virtual orbitals and hence stabilization is small according to the populations in Tables 3 and 5, presumably because these orbitals lie at too high energy.

The $\Delta E(A_{1g})$ and $\Delta E(E_u)$ terms are found to give instead a quite relevant contribution to the σ-bond, reflecting the large charge transfers into 4s and $4p_\sigma$ respectively by ring orbitals. These terms, similarly to $\Delta E(B_{2g})$, do not show a regular trend along the metallophthalocyanine series, although here the energies differ much less from one metal to another. According to Table 6, both the $\Delta E(A_{1g})$ and $\Delta E(E_u)$ terms do not differ significantly on going from NiPc to NiP.

Out-of-Plane (π) Bonding. As for the energy terms which account for the π-bond, the $\Delta E(A_{2u})$ is small, but not negligible, due to the fact that this term also contains, apart from the contribution due to interaction of π orbitals of the ring with $4p_z$, a contribution due to polarization of the macrocycle.

The only significant contribution to the π-bond derives from the $\Delta E(E_g)$ term. It would be misleading however to interpret

this term as a measure of the strength of the π-back-donation from d_π into the empty Pc- or P-π^* orbitals, because as inferred by the charge transfers that occur in this symmetry (see Table 3) polarization effects are quite important. Although we cannot distinguish charge transfer and polarization in the $\Delta E(E_g)$ energy term, nevertheless some suggestions can be made. The constancy of the $\Delta E(E_g)$ energy term in spite of the difference (ca. 0.15 electron) in the charge donated by Cu d_π orbitals on one hand and cobalt and nickel on the other hand, suggests that polarization of the macrocycle is energetically more important than charge transfer. In MgPc where π back-donation is not present and $\Delta E(E_g)$ accounts almost exclusively for polarization effects, this term is only ~0.4 eV smaller than in transition metal phthalocyanines.

Summary. The detailed analysis above of the different contributions to ΔE_{oi} points out that, as concerns MPc's (M = Co, Ni, Cu) and NiP, (i) the σ-interactions are by far dominant and account for most of the bond strength, (ii) polarization of the ring makes an important contribution, (iii) π back-donation gives only a minor energetic contribution to the metal–macrocycle bond, and (iv) bonding in NiP is slightly stronger than in NiPc due to a more negative steric term caused by both a smaller Pauli repulsion and a stronger electrostatic attraction. The orbital interactions in NiP are in general very similar although slightly weaker than in NiPc.

Comparison with MgPc. Comparing now MgPc to the transition metal phthalocyanines, it is immediately apparent from Table 6 that the $\Delta E(B_{2g})$ term, that in transition metal phthalocyanines gives the major contribution to the bond, is now strikingly small, due of course to the poor σ acceptor capability of the $3d_{xy}$ of Mg. The energy terms which account for the interactions with 3s and 3p orbitals, i.e. $\Delta E(A_{1g})$ (3s), $\Delta E(A_{2u})$ ($3p_z$), and $\Delta E(E_u)$ ($3p_\sigma$), do not differ to such a large extent. Compared to those for transition metal analogues, these terms are in general smaller in MgPc. This less effective interaction can be ascribed to the larger hole size and to a less favourable energy matching between Mg and Pc orbitals. The overall decrease of the orbital interaction terms, but mostly the drop of the $\Delta E(B_{2g})$, is reflected in the total ΔE_{oi}, which is in MgPc only half of that computed for the transition metal phthalocyanines. This result unequivocally demonstrates, that, although s and p orbitals play a role in the metal–macrocycle bond, the TM 3d orbitals are much more important.

Ionic versus Covalent Bonding. Finally we will comment on the relative importance of steric and orbital interaction contributions to the bond in these systems. From the energy decomposition of Table 6 we find that the ΔE_{oi} term is stabilizing in all investigated systems, but it is invariably smaller than the steric term, ΔE^0, although by an amount that changes considerably from one compound to another. If we consider the steric term, ΔE^0 as a measure of the "ionic" contribution to the bonding, our results show that in transition metal phthalocyanines ionic and covalent contributions to the bond are roughly the same. Formation of MgPc from Mg^{2+} and Pc^{2-} is primarily an ionic process because ΔE_{oi} is relatively weak (–8.77 eV) and represents only one-third of the total bonding energy ($\Delta E_{oi} + \Delta E^0$), which is 27.63 eV. Thus, our quantitative results on MgPc fully corroborate previous suggestions based on extended Hückel calculations,[41,51] that alkaline earth complexes of tetrapyrrole ligands show, compared to transition metal analogues, an increased importance of ionic metal to macrocycle bonding.

4. Spectroscopy of Metallophthalocyanines

(a) Photoelectron Spectra. The ultraviolet photoelectron spectra of metal-free phthalocyanine and some MPc's (M = Mg, Fe, Co, Ni, Cu, Zn) obtained for the gaseous molecules by Berkowitz[13] display almost identical features from one phthalocyanine to another. They show a narrow peak with a higher energy shoulder at ~6.4 eV, followed by a rather broad band beginning at ~8 eV that exhibits fine structure more readily apparent in some compounds than others, and then a higher energy region from ~10 to 14.5 eV characterized by broad, fairly intense, and interspersed structure. Previous UV photoemission studies[10,11] of these compounds, from thin films, gave analogous results. Although weak contributions of the central metal d-electrons can be identified, the spectra are at first order identical for all Pc's and represent essentially the π-electron ring system. They appear to be a superposition of the spectra of benzene and an inner porphyrin skeleton. Surprisingly, the spectral features do not change in varying the incident photon energy from 21.2 to 40.8 eV. Battye *et al.*[11] interpret this as a result of relatively low partial cross sections for photoionization of metal d-like orbitals, not only at 21.2 but also at 40.8 eV. However, the AlK ($h\nu$ = 1486.7 eV) thin film spectra of Höchst *et al.*[12] in the range 0–6 eV differ considerably from one phthalocyanine to another and show increasing relative intensity with increasing number of d electrons, which is evidence that the prominent spectral features correspond to the d states. This behavior has been supposed to be related to the fact that these orbitals have a relatively higher cross section than the ring orbitals in the X-ray region. We present in Table 7 the results of DF calculations on the ionization spectra of the MPc series (M = Mg, Ni, Co, Cu) together with the vertical ionization energies derived from UPS experiments,[13] which are the most appropriate for comparison. The ionization potentials derived from XPS spectra are in fact referred to the Fermi energy and hence cannot be directly compared to molecular calculations, although they give useful indications on the relative energies of d states.

In order to fully include relaxation effects which are relevant when the ionization process involves highly localized orbitals, as in the case of metal d orbitals, we used the ΔSCF procedure. The ionization energies of the open shell systems, CoPc and CuPc, have been obtained by spin unrestricted calculations and the energies of the resulting singlet and triplet spin components are reported in Table 7 for the orbitals that give significant splitting. Note that significant singlet–triplet splittings occur only in cases where the two unpaired electrons are in d states.

From our calculations the general spectral pattern is very similar for all MPc's: a first ionization computed at ~6 eV followed by a second ionization ~0.7 eV higher and then a 0.4-eV gap preceding a number of higher ionizations very close in energy. In MgPc this gap is very small, so it would be more appropriate in this case to describe the theoretical spectral pattern in terms of a first ionization followed by an onset of higher ionizations starting at ~1.2 eV higher energy. According to our calculations, the sharp peak at ~6.4 eV originates from $(2a_{1u})^{-1}$, which we find to be the lowest ionization in all MPc's. Although the computed value is somewhat lower than the experimental one, particularly in MgPc and NiPc, this assignment is quite unambiguous. The fact that the first ionization occurs invariably at ~6.4 eV in all MPc's and in the metal-free phthalocyanine as well can be explained only in terms of ionization from a ring orbital. The $2a_{1u}$ is the obvious candidate.

The energy of the next computed ionization, in the transition metal complexes, fits in with the assignment of this ionization to the experimental shoulder. Although this assignment cannot be regarded as conclusive, it is quite reasonable that this ionization gives a weak spectral feature in the UV region as it involves molecular orbitals largely metallic in nature, i.e. the $6e_g$ (d_π) in the case of cobalt and nickel and the $11b_{2g}$ (d_{xy}) in the case of the copper, with low partial cross section.

It is hard to assign specific computed ionizations to the few distinguishable features shown by the two next broad bands spanning the regions ~8–9 and ~10–14.5 eV. However, we will

(51) Zerner, M.; Gouterman, M. *Theor. Chim. Acta* **1967**, *8*, 26.

Table 7. Calculated and Experimental Ionizations for MPc's (M = Mg, Co, Ni, Cu), Where for CoPc and NiPc the Singlet and Triplet Spin Components Are Given for the Orbitals That Give a Significant Splitting

MgPc			CoPc			NiPc			CuPc		
MO	calcd	exptl[a]	MO	calcd	exptl[a]	MO	calcd	exptl[a]	MO	calcd	exptl[a]
$2a_{1u}$	5.88	6.35 s	$2a_{1u}$	6.00	6.38 s	$2a_{1u}$	5.80	6.38 s	$2a_{1u}$	6.00	6.38 s
$3b_{1u}$	7.03	~6.50 sh	$6e_g$ (d)	6.78	6.57 sh	$6e_g$(d)	6.68	6.55 sh	$11b_{2g}$(d)	6.61	sh
				6.65							
$4e_g$	7.16		$9b_{1g}$(d)	7.05		$5a_{2u}$	7.18		$6e_g$	7.05	
$5a_{2u}$	7.17		$3b_{1u}$	7.23		$3b_{1u}$	7.22		$3b_{1u}$	7.10	
$5e_g$	7.18		$5a_{2u}$	7.29		$5e_g$	7.28		$5a_{2u}$	7.28	
$8b_{1g}$	7.21		$5e_g$	7.34		$2b_{2u}$	7.33		$9b_{1g}$	7.30	7.45 pw
$2b_{2u}$	7.31		$2b_{2u}$	7.42		$9b_{1g}$	7.40		$5e_g$	7.49	
$4a_{2u}$	7.58		$19e_u$	7.88		$19e_u$	7.82		$2b_{2u}$	7.54	
$19e_u$	7.59		$4a_{2u}$	7.91		$13a_{1g}$(d)	7.85	7.75 dp	$19e_u$	7.77	
$1a_{1u}$	7.79		$13a_{1g}$ (d)	7.96		$4a_{2u}$	7.92		$4a_{2u}$	7.88	
										7.78	
$12a_g$	8.27	8.36 b	$1a_{1u}$	7.99		$1a_{1u}$	8.00		$1a_{1u}$	8.04	
$10b_{2g}$	8.56	8.63 b	$4e_g$	8.17		$4e_g$	8.05		$13a_{1g}$	8.47	
				7.92				8.44		8.31	
$5e_g$	8.98	8.81 b	$12a_{1g}$	8.58		$12a_{1g}$	8.47		$4e_g$(d)	8.92	
					8.83 b			8.81		8.89	8.79
			$8b_{1g}$(d)	8.73		$8b_{1g}$(d)	9.39	9.10 sh	$18e_u$	9.59	
				8.14							9.39 sh
									$3e_g$	9.96	
										9.84	
			$3e_g$	9.33		$3e_g$	9.40		$18e_u$	9.59	
			$10b_{2g}$	9.55		$10b_{2g}$	9.61		$8b_{1g}$(d)	10.17	
										9.99	
											10.26 pw
			$18e_u$	9.68		$18e_u$	9.73		$12a_{1g}$(d)	10.99	
										8.25	8.31 sh
											11.40 b
									$10b_{2g}$	11.28	
										10.80	

[a] Vapor phase photoelectron spectra. [13] notation is s = sharp, sh = shoulder, b = broad, pw = possible weak peak, dp = distinct peak.

attempt to locate those features which, on theoretical grounds, might be due to photoionizations from metal 3d-like orbitals.

In the case of CoPc the broad band at 8.83 eV in the UPS spectrum does not exhibit fine structure, so the only available experimental evidence for the d states is provided by the XPS thin film work,[12] according to which the CoPc spectrum shows two d band structures separated by less than 2 eV. We compute four 3d-like ionizations, i.e., the $(6e_g)^{-1}$, $(9b_{1g})^{-1}$, $(13a_{1g})^{-1}$, and $(8b_{1g})^{-1}$. The $9b_{1g}$ and $8b_{1g}$ should be both considered as metallic states as they are composed, in CoPc, of metal $3d_{x^2-y^2}$ and ligand in almost equal amount. On the basis of their relative energies the $(6e_g)^{-1}$ and $(9b_{1g})^{-1}$ could be responsible for the first of the two experimental bands, while the higher energy band most likely contains the $(13a_{1g})^{-1}$ and $(8b_{1g})^{-1}$ IPs. The computed energy gap between the two IP sets agrees fairly well with the experimental one, taking into account the fact that, due to the large spin splitting, one spin component of the $(8b_{1g})^{-1}$ falls at 8.73 eV, at ~2 eV higher energy than the first ionization, the $(6e_g)^{-1}$.

As concerns NiPc, the ionizations that correspond to metallic states, i.e. $(6e_g)^{-1}$, $(13a_{1g})^{-1}$, and $(8b_{1g})^{-1}$ are computed respectively at 6.68, 7.85, and 9.39 eV. Their energies fit in with the assignment of these ionizations to the shoulder at ~6.55, the deep peak at 7.75 and the shoulder at 9.10 eV of the UV gas-phase spectrum. Berkowitz, by comparison with the XPS spectrum tentatively identifies as 3d-like ionizations the features at 7.75, 8.44, and 9.10 eV of the UV gas phase spectrum. Our calculations support the assignment of the features at 7.75 and 9.10 eV to 3d-like ionizations, but exclude the feature at 8.44 eV as ionization characteristic of metal 3d-like orbitals.

According to our calculations, the copper d-like ionizations consist of $(11b_{2g})^{-1}$, $(4e_g)^{-1}$, $(8b_{1g})^{-1}$, and $(12a_{1g})^{-1}$. The first falls at 6.61 eV, while the last three, considering the two spin components, span the region 8.25–10.99 eV. The X-ray spectrum of CuPc displays a very broad and intense peak at ~6 eV and a much less intense peak at about 3.5 eV higher energy. Höchst *et al.*[12] interpret tentatively the outermost peak as produced by photoemission from $b_{2g}(d_{xy})$ orbital and the broad peak as due to photoionization from the states $e_g(d_\pi)$, $b_{1g}(d_{x^2-y^2})$, $a_{1g}(d_{z^2})$. This view is supported by our theoretical results which reproduce quite well the observed spectral pattern.

The location of d-like features in the UV gas-phase spectrum is, for the above discussed reasons, very difficult on experimental grounds alone. In fact, except for a broad band centered at ~11.4 eV which looks somewhat more intense in the 40.8-eV spectrum and is weak or absent in the metal-free H_2Pc, there are no more features which can be diagnostics for the energy location of metal d-like orbitals. Berkowitz, however, comparing similar features in UV and XPS spectra, suggests that the broad band at ~11.4 eV together with the weak peak at 7.45 eV might correspond to the two prominent features of the XPS thin film spectrum and then identifies these features as metal d-like in nature. Our calculations indicate that the broad band with the maximum at ~11.4 eV most likely originates from the highest energy spin components of the states $(8b_{1g})^{-1}$ and $(12a_{1g})^{-1}$, supporting the identification of this band as metal d-like in origin, whereas the feature at 7.45 cannot be assigned to the $(11b_{2g})^{-1}$ ionization that is computed more than 1 eV lower (6.61 eV). According to our theoretical results, the spectroscopical features at 8.31, 8.79 closely correspond to metal d-like ionizations, i.e. the lowest energy spin component of the state $(12a_{1g})^{-1}$ and the two spin components of the state $(4e_g)^{-1}$ computed respectively at 8.25, 8.92, and 8.89 eV.

Although the assignments of the d-like ionizations that we give may not be conclusive, it is encouraging that both theoretical and experimental results clearly indicate an increase of the binding energy for the 3d-like orbitals on going from CoPc to CuPc.

(b) Optical Spectra. The optical properties of phthalocyanines have been experimentally investigated in the vapor phase,[15] in organic solutions,[15] in thin films,[16,17] and in single crystals.[14,52]

(52) Heagy, M. D.; Rende, D. E.; Shaffer, G. W.; Wolfe, B. M.; Liou, K.; Hoffman, B. M.; Musselman, R. L. *Inorg. Chem.* **1989**, *28*, 283.

Table 8. Calculated and Experimental Optical Transitions for CoPc (Transition Energies Given in Units of 10^3 cm^{-1})

			exptl[15]	
type	transitions	theor ϵ	notation	ϵ
$\pi(C) \rightarrow \pi(C,N), d_\pi$	$2a_{1u} \rightarrow 7e_g$	12.76	Q	15.22
$\pi(C,N_b) \rightarrow \pi(C,N), d_\pi$	$5a_{2u} \rightarrow 7e_g$	23.70	EB[a]	17.88
$\pi(C,N_p) \rightarrow \pi(C,N), d_\pi$	$3b_{1u} \rightarrow 7e_g$	23.78		
$\pi(C) \rightarrow \pi(C,N), d_\pi$	$2b_{2u} \rightarrow 7e_g$	24.10	EB	20.83
$\sigma(N_b), d_{x^2-y^2} \rightarrow d_{xy}$	$9b_{1g} \rightarrow 11b_{2g}$	25.48		
$d_\pi \rightarrow d_{xy}$	$6e_g \rightarrow 11b_{2g}$	26.44		
$\pi(N) \rightarrow \pi(C,N), d_\pi$	$4a_{2u} \rightarrow 7e_g$	26.87		
$\pi(C) \rightarrow \pi(C)$	$2a_{1u} \rightarrow 8e_g$	28.65		
$\pi(C) \rightarrow \pi(C,N), d_\pi$	$1a_{1u} \rightarrow 7e_g$	30.02		
$d_\pi \rightarrow \pi(C,N_b)$	$6e_g \rightarrow 3b_{2u}$	30.61		
$d_\pi \rightarrow \pi(C,N_p)$	$6e_g \rightarrow 4b_{1u}$	31.72	B	32.00
$d_{z^2} \rightarrow d_{xy}$	$13a_{1g} \rightarrow 11b_{2g}$	32.56		
$d_\pi \rightarrow \pi(C)$	$6e_g \rightarrow 6a_{2u}$	34.10		
$\pi(C) \rightarrow \pi(C,N_b)$	$5e_g \rightarrow 3b_{2u}$	34.73		
$\sigma(N_b), d_{x^2-y^2} \rightarrow \pi(C,N_b)$	$9b_{1g} \rightarrow 3b_{2u}$	35.49		
$\pi(C) \rightarrow \pi(C,N_p)$	$5e_g \rightarrow 4b_{1u}$	36.55	EB	36.36
$\pi(N_b) \rightarrow d_{xy}$	$19e_u \rightarrow 11b_{2g}$	37.00		
$\pi(C,N_p) \rightarrow \pi(C)$	$3b_{1u} \rightarrow 8e_g$	39.01		
$\pi(C) \rightarrow \pi(C)$	$5e_g \rightarrow 6a_{2u}$	39.11		
$\pi(C,N_b) \rightarrow \pi(C)$	$5a_{2u} \rightarrow 8e_g$	39.30		
$\pi(C) \rightarrow \pi(C)$	$2a_{1u} \rightarrow 9e_g$	39.73		
$\pi(C) \rightarrow \pi(C)$	$2b_{2u} \rightarrow 8e_g$	39.89	L	41.67
$\pi(C,N_p), d_\pi \rightarrow \pi(C,N_b)$	$4e_g \rightarrow 3b_{2u}$	40.00		
$\pi(C,N_p), d_\pi \rightarrow \pi(C,N_p)$	$4e_g \rightarrow 4b_{1u}$	41.48		
$d_{z^2} \rightarrow \pi(C)$	$13a_{1g} \rightarrow 6a_{2u}$	43.41		
$\sigma(N_b), d_{x^2-y^2} \rightarrow \pi(C,N_b)$	$8b_{1g} \rightarrow 3b_{2u}$	43.45		
$\pi(N) \rightarrow \pi(C)$	$4a_{2u} \rightarrow 8e_g$	44.11		
$\pi(C) \rightarrow \pi(C)$	$1a_{1u} \rightarrow 8e_g$	44.60		
$\pi(C) \rightarrow \pi(C,N), d_\pi$	$3a_{2u} \rightarrow 7e_g$	45.53		
$d_\pi \rightarrow \pi(C)$	$6e_g \rightarrow 3a_{1u}$	46.05	C	47.62

[a] "Extra bands".

Table 9. Calculated and Experimental Optical Transitions for NiPc (Transition Energies Given in Units of 10^3 cm^{-1})

			exptl[15]	
type	transitions	theor ϵ	notation	ϵ
$\pi(C) \rightarrow \pi(C,N), d_\pi$	$2a_{1u} \rightarrow 7e_g$	13.00	Q	15.36
$d_\pi \rightarrow d_{xy}$	$6e_g \rightarrow 11b_{2g}$	21.87		
$\pi(C) \rightarrow \pi(C,N), d_\pi$	$2b_{2u} \rightarrow 7e_g$	23.79	EB[a]	19.23
$\pi(C,N_b) \rightarrow \pi(C,N), d_\pi$	$5a_{2u} \rightarrow 7e_g$	24.89		
$\pi(C,N_p) \rightarrow \pi(C,N), d_\pi$	$3b_{1u} \rightarrow 7e_g$	24.42		
$d_{z^2} \rightarrow d_{xy}$	$13a_{1g} \rightarrow 11b_{2g}$	25.87		
$\pi(N) \rightarrow \pi(C,N), d_\pi$	$4a_{2u} \rightarrow 7e_g$	27.85		
$\pi(C) \rightarrow \pi(C)$	$2a_{1u} \rightarrow 8e_g$	29.14		
$\pi(C) \rightarrow \pi(C,N), d_\pi$	$1a_{1u} \rightarrow 7e_g$	30.14		
$d_\pi \rightarrow \pi(C,N_b)$	$6e_g \rightarrow 3b_{2u}$	32.40		
$d_\pi \rightarrow \pi(C,N_p)$	$6e_g \rightarrow 4b_{1u}$	32.57	B	30.53
$d_{x^2-y^2} \rightarrow d_{xy}$	$8b_{1g} \rightarrow 11b_{2g}$	32.69		
$\pi(N_b) \rightarrow d_{xy}$	$19e_u \rightarrow 11b_{2g}$	34.53		
$d_\pi \rightarrow \pi(C)$	$6e_g \rightarrow 6a_{2u}$	35.73		
$\sigma(N_b), d_{x^2-y^2} \rightarrow \pi(C,N_b)$	$9b_{1g} \rightarrow 3b_{2u}$	36.82		
$\pi(C) \rightarrow \pi(C,N_p)$	$5e_g \rightarrow 4b_{1u}$	37.40	EB	35.21
$\pi(C) \rightarrow \pi(C,N_b)$	$5e_g \rightarrow 3b_{2u}$	37.56		
$\pi(N) \rightarrow \pi(C)$	$4a_{2u} \rightarrow 8e_g$	39.12		
$\pi(C) \rightarrow \pi(C)$	$2a_{1u} \rightarrow 9e_g$	39.28		
$\pi(C) \rightarrow \pi(C)$	$5e_g \rightarrow 6a_{2u}$	39.72		
$\pi(C,N_p) \rightarrow \pi(C)$	$3b_{1u} \rightarrow 8e_g$	39.89	L	42.55
$\pi(C) \rightarrow \pi(C)$	$2b_{2u} \rightarrow 8e_g$	40.62		
$\pi(C,N_b) \rightarrow \pi(C)$	$5a_{2u} \rightarrow 8e_g$	40.63	EB	42.55
$\pi(C,N_p), d_\pi \rightarrow \pi(C,N_b)$	$4e_g \rightarrow 3b_{2u}$	42.59		
$\pi(C,N_p), d_\pi \rightarrow \pi(C,N_p)$	$4e_g \rightarrow 4b_{1u}$	43.03		
$d_{z^2} \rightarrow \pi(C)$	$13a_{1g} \rightarrow 6a_{2u}$	43.57	EB	45.87
$\pi(C) \rightarrow \pi(C)$	$1a_{1u} \rightarrow 8e_g$	45.40		
$d_\pi \rightarrow \pi(C)$	$6e_g \rightarrow 3a_{1u}$	46.17	C	47.62
$\pi(C) \rightarrow \pi(C,N), d_\pi$	$3a_{2u} \rightarrow 7e_g$	47.02		
$d_{x^2-y^2} \rightarrow \pi(C,N_b)$	$8b_{1g} \rightarrow 3b_{2u}$	49.79		

[a] "Extra bands".

As major spectral features the bands Q, B, N, L, and C have been identified, which are found in the vapor spectra in the regions 15.2, 31.3, 36.4, 40.8, and 47.6 kcm^{-1}. In addition to these five bands characteristic of the phthalocyanine ring, "extra" bands that appear to be metal dependent have been located in the vapor and solid-state spectra of some MPc's, e.g. CoPc and NiPc. The UV/vis spectroscopy of porphyrins and their derivatives has been for long time interpreted on the basis of the simple Gouterman four orbital model.[53-55] According to this model, the B and Q bands can be explained in terms of excitations involving four orbitals, the occupied a_{1u} and a_{2u} and the empty doubly degenerate e_g orbitals. In porphyrins, the near degeneracy of the $a_{1u}{}^1e_g{}^1$ and $a_{2u}{}^1e_g{}^1$ excited configurations (cf. the proximity of $4a_{2u}$ and $1a_{1u}$ in NiP, Figure 6) leads to a strong configuration interaction that results in the B state being $\sim 15.0 \times 10^3$ cm^{-1} above the Q state, in fair agreement with experiment. Furthermore, due to the configuration mixing, the Soret or B band contains nearly all the intensity while the Q band is weak, which is consistent with a Q band being about $^1/_{10}$th the intensity of the B band, unlike in phthalocyanines where the B and Q bands have about the same intensity. The reason for this difference is, as shown by extended Hückel calculations, the larger gap between the a_{1u} and a_{2u} orbitals in phthalocyanines compared to porphyrins (cf. also the large gap between $2a_{1u}$ and $4a_{2u}$ in our MPc calculation, Figure 2) that eliminates CI for the $a_{1u}{}^1e_g{}^1$ and $a_{2u}{}^1e_g{}^1$ excited configurations and consequently the forbidden character of the lower energy transition, so that the Q band is no longer weak. Gouterman[54] assigned the visible Q transition as pure $a_{1u} \rightarrow e_g$ and the ultraviolet B transition as pure $a_{2u} \rightarrow e_g$.

Later, Henriksson et al.[43,56] interpreted the optical spectra of CuPc and H_2Pc using a more elaborate semiempirical model, and suggested that several electronic transitions are responsible for the characteristic B, Q, N, L, and C spectral features. This model also revealed the importance of n-π^* transitions from inner and bridge nitrogens as well as metal–ligand charge transfer in the optical region. Recently, Liang et al.,[4] using first principles local density theory, have provided an analysis of the optical transitions of some MPc's that largely supports the interpretation of the Pc's spectral features given by Henriksson.[43,56]

We present here a DF investigation of the optical spectra of the MPc series (M = Co, Ni, Cu) performed using more sophisticated density functionals for exchange and correlation (see section 2) in which a nonlocal correction according to Becke[24] is added to the Xα exchange and the correlation is treated in the Vosko–Wilk–Nusair parametrization,[22] with a correction of Stoll et al.[23] The final-state relaxation effects were also fully included by using the ΔSCF procedure. The results of these calculations are given in Tables 8–10 for CoPc, NiPc, and CuPc respectively and are compared with the experimental vapor phase absorptions.[15]

We have not computed singlet–triplet splittings for any of the three metallophthalocyanines, however, as we have already seen in the photoionizations, they are expected to be significant only in cases where the two unpaired electrons are in d states. Anyway, the limited resolution of the experimental spectra would preclude any comparison to calculated splittings. Our results show the lowest energy transition to be a $2a_{1u} \rightarrow 7e_g$ in all three MPc's. Its energy differs very little from one phthalocyanine to another and is very close to the experimental so-called Q band, which is consistent with previous[4,43] assignment of this peak to the strong $2a_{1u} \rightarrow 7e_g$ transition. Both vapor and single-crystal spectra of MPc's show a shoulder on the high energy side of the Q band that has been supposed[15] to be a vibronic component of the band. More recent experimental[57-59] and theoretical studies[4,43] have

(53) Gouterman, M. *J. Mol. Spectrosc.* **1961**, *6*, 138.
(54) Gouterman, M. In *The Porphyrins*; Dolphin, D., Ed.; Academic Press: New York, 1978; pp 1–166.
(55) Wang, M.-Y. R.; Hoffman, B. M. *J. Am. Chem. Soc.* **1984**, *106*, 4235.
(56) Henriksson, A.; Roos, B.; Sundbom, M. *Theor. Chim. Acta* **1972**, *27*, 213.
(57) Fitch, P. M.; Sharton, L.; Levy, D. H. *J. Chem. Phys.* **1979**, *70*, 2018.
(58) Metcalf, D. H.; VanCott, T. C.; Snyder, S. W.; Schatz, P. N.; Williamson, B. E. *J. Phys. Chem.* **1990**, *94*, 2828.

Table 10. Calculated and Experimental Optical Transitions for CuPc (Transition Energies Given in Units of 10^3 cm^{-1})

			exptl[15]	
type	transitions	theor ϵ	notation	ϵ
$\pi(C) \rightarrow \pi(C,N)$	$2a_{1u} \rightarrow 7e_g$	12.82	Q	15.21
$\pi(C,N_p) \rightarrow \pi(C,N)$	$3b_{1u} \rightarrow 7e_g$	22.71		
$\pi(C,N_b) \rightarrow \pi(C,N)$	$5a_{2u} \rightarrow 7e_g$	23.33		
$\pi(N) \rightarrow \pi(C,N)$	$4a_{2u} \rightarrow 7e_g$	26.28		
$\pi(C) \rightarrow \pi(C,N)$	$2b_{2u} \rightarrow 7e_g$	26.82		
$\pi(N_b) \rightarrow d_{xy}$	$19e_u \rightarrow 11b_{2g}$	27.96		
$d_{z^2} \rightarrow d_{xy}$	$13a_{1g} \rightarrow 11b_{2g}$	28.09 23.1[a]		
$d_\pi \rightarrow d_{xy}$	$4e_g \rightarrow 11b_{2g}$	29.29 23.3[a]		
$\pi(C) \rightarrow \pi(C)$	$2a_{1u} \rightarrow 8e_g$	30.08		
$\pi(C) \rightarrow \pi(C,N)$	$1a_{1u} \rightarrow 7e_g$	30.29		
$d_{x^2-y^2} \rightarrow d_{xy}$	$8b_{1g} \rightarrow 11b_{2g}$	32.51 26.8[a]		
$\pi(C,N_p), d_\pi \rightarrow \pi(C,N_b)$	$6e_g \rightarrow 3b_{2u}$	33.41		
$\pi(C,N_p), d_\pi \rightarrow \pi(C,N_p)$	$6e_g \rightarrow 4b_{1u}$	35.56	B	30.77
$\pi(C) \rightarrow \pi(C,N_b)$	$5e_g \rightarrow 3b_{2u}$	37.07		
$\pi(C,N_p), d_\pi \rightarrow \pi(C)$	$6e_g \rightarrow 6a_{2u}$	37.85	N	36.23
$\pi(C) \rightarrow \pi(C,N_p)$	$5e_g \rightarrow 4b_{1u}$	38.99		
$\pi(C,N_p) \rightarrow \pi(C)$	$3b_{1u} \rightarrow 8e_g$	39.05		
$\pi(C) \rightarrow \pi(C)$	$2a_{1u} \rightarrow 9e_g$	39.40		
$\pi(C,N_b) \rightarrow \pi(C)$	$5a_{2u} \rightarrow 8e_g$	39.86		
$\pi(C) \rightarrow \pi(C)$	$5e_g \rightarrow 6a_{2u}$	40.77		
$d_\pi \rightarrow \pi(C,N_b)$	$4e_g \rightarrow 3b_{2u}$	41.12		
$\pi(C) \rightarrow \pi(C)$	$2b_{2u} \rightarrow 8e_g$	41.83	L	41.58
$d_\pi \rightarrow \pi(C,N_p)$	$4e_g \rightarrow 4b_{1u}$	43.54		
$\pi(N) \rightarrow \pi(C)$	$4a_{2u} \rightarrow 8e_g$	44.94		
$\pi(C) \rightarrow \pi(C)$	$1a_{1u} \rightarrow 8e_g$	45.79		
$\pi(C) \rightarrow \pi(C,N), d_\pi$	$3a_{2u} \rightarrow 7e_g$	45.97		
$\pi(C,N_p), d_\pi \rightarrow \pi(C)$	$6e_g \rightarrow 3a_{1u}$	47.08	C	45.87

[a] d–d transitions computed by Henriksson et al. (see ref 43).

proposed that at least an additional electronic transition resides in the high energy shadow of peak Q and have suggested to interpret the blue shoulder of this peak as due to a combination of overtones from Q and an additional electronic transition.

Henriksson[43] indicates as responsible for the observed blue shoulder two weakly allowed doublets, the π–π^* ^2E_u (21.6 kcm^{-1}) and the n–π^* $^2B_{2u}$ (22.0 kcm^{-1}), while Liang et al.[4] assign it to the relatively intense $5a_{2u} \rightarrow 7e_g$ transition. Our calculations seem to support the latter assignment. We find this transition in CoPc, NiPc, and CuPc at 23.70×10^3, 24.89×10^3, and 23.33×10^3 cm^{-1} respectively, to be compared with 22.27×10^3, 21.97×10^3, and 15.41×10^3 cm^{-1} computed by Liang.[4] Although their energies are somewhat lower than ours, in the case of CuPc their energy of the $5a_{2u} \rightarrow 7e_g$ transition appears to be anomalously low and out of the trend.

In addition to $5a_{2u} \rightarrow 7e_g$, at least one other allowed π–π^* transition falls in the high energy shadow of peak Q. In this region, CoPc and NiPc show also weak "extra" bands at 17.9×10^3 and 20.8×10^3 cm^{-1} and 19.2×10^3 cm^{-1}, respectively. It is tempting to interpret these features as largely due to the d–d transitions at 25.5×10^3 and 26.4×10^3 cm^{-1} in the case of the cobalt and at 21.9×10^3 and 25.9×10^3 cm^{-1} in the case of the nickel. This assignment would also be consistent with the metal dependent character of these "extra" bands suggested by Gouterman.[15]

As concerns the strong absorption in the near-UV region, the so-called Soret band, we predict at least five allowed transitions in this region, in contrast with Gouterman's[15] suggestion that the B band originates from the $5a_{2u} \rightarrow 7e_g$ transition. Calculations by Henriksson et al.[43] on CuPc indicate that this band has a more complicated structure than the Q band. They attribute to the B band two intense $\pi \rightarrow \pi^*$ transitions calculated at 34.5×10^3 and 35.3×10^3 cm^{-1} and three weakly allowed transitions, an n $\rightarrow$ π^* at the low energy side (calculated at 31.4×10^3 cm^{-1}), and two $\pi \rightarrow \pi^*$ transitions calculated at 34.4×10^3 and 36.6×10^3 cm^{-1}. Recent investigation by Liand et al.[4] also agrees with our findings that more than one transition is responsible for the Soret band. The $1a_{1u} \rightarrow 7e_g$, $2a_{1u} \rightarrow 8e_g$, and $4a_{2u} \rightarrow 7e_g$ $\pi \rightarrow \pi^*$ transitions fall in the low-energy region of the B band in all molecules of the series.

In the same region CuPc shows two additional allowed transitions, the $\pi \rightarrow \pi^*$ $2b_{2u} \rightarrow 7e_g$ and the n $\rightarrow$ d (from the nitrogen bridge lone pair) $19e_u \rightarrow 11b_{2g}$. In CoPc and NiPc, these transitions are respectively red and blue shifted, so, while the $2b_{2u} \rightarrow 7e_g$ falls in the Q-band region, the $19e_u \rightarrow 11b_{2g}$ may contribute to the "extra" band observed in the high-UV region. Furthermore, very close to the experimental maximum of the Soret band occur the $6e_g \rightarrow 3b_{2u}$ and the $6e_g \rightarrow 4b_{1u}$, transitions. The latter is predicted by Liang et al.[4] to be uniformly intense and close to 32×10^3 cm^{-1} in all molecules of the MPc series (M = Co, Ni, Cu), and has been considered as the main transition responsible for the B band. From our calculations the blue shift of both transitions when going from cobalt to copper is clearly distinguishable, but not uniform, being particularly large in CuPc. This is not surprising in the light of the different nature of the $6e_g$ orbital within the members of the series. Thus, while in the case of CuPc these transitions are almost pure $\pi \rightarrow \pi^*$ (the $6e_g$ orbital only contains a minor d_π character), in the case of CoPc and NiPc they should be classified as MLCT in view of the large d_π character of the $6e_g$ orbital.

As shown in Table 10, in the region of the B band, our calculations also predict three d–d transitions for CuPc, in close agreement with results by Henriksson et al.[43] In the same region, somewhat higher in energy, an additional d–d transition is also predicted for CoPc and NiPc, indicating that overall the d–d transitions underlies both Q and B bands in the investigated MPc's.

The remainder of the UV absorptions, i.e. bands N, L, and C, also are predicted by our calculations to be due to several transitions, in accordance with previous[4,43] theoretical results. Although the high-UV region of the spectra is largely characterized by $\pi \rightarrow \pi^*$ transitions, a number of d $\rightarrow$ π^* transitions are also predicted in this region, particularly for CoPc and NiPc. Unlike CuPc, they present in the high-UV region very intense "extra" bands, in addition or in place of the usual N, L, and C features. The metal dependent nature of these "extra" bands is nicely confirmed by our calculations, as shown in Tables 8 and 9. The d $\rightarrow$ π^* transitions $6e_g \rightarrow 6a_{2u}$ and $9b_{1g} \rightarrow 3b_{2u}$ for instance are both in CoPc and NiPc fairly close to the "extra" bands at 36.36×10^3 and 35.2×10^3 cm^{-1}, respectively.

Acknowledgment. We are grateful to Mr. P. Vernooijs for his help with the calculations.

(59) Rende, D. E.; Heagy, M. D.; Heuer, W. B.; Liou, K.; Thompson, J. A.; Hoffman, B. M.; Musselman, R. L. *Inorg. Chem.* **1992**, *31*, 352.